UNIVERSIDAD NACIONAL DE COLOMBIA

Analysis of mechanisms of phytoplankton layer formation, maintenance and dissipation in a tropical reservoir

Oscar Dario Beltrán Perez

Universidad Nacional de Colombia

Facultad de Minas, Departamento de Geociencias y Medio Ambiente

Medellín, Colombia

2017

Analysis of mechanisms of phytoplankton layer formation, maintenance and dissipation in a tropical reservoir

Oscar Dario Beltrán Perez

A thesis submitted in partial fulfillment of the requirements for the degree of

Master of Engineering in Water Resources

Advisor:

Francisco Mauricio Toro Botero, Ph.D.

Co-advisor:

Evelio Andrés Gómez Giraldo, Ph.D.

Research field:

Water quality

Research group:

Posgrado en Aprovechamiento de Recursos Hidráulicos

Universidad Nacional de Colombia

Facultad de Minas, Departamento de Geociencias y Medio Ambiente

Medellín, Colombia

2017

Do not let the day end without having grown a bit,
without being happy,
without having risen your dreams.

Fragment of Carpe Diem by Walt Whitman.

Acknowledgments

Thanks first of all to God for the gift of life and for allowing me to finish this step in my live. A special thanks goes to my wife for all her support in the bad and good moments, without her unconditional love, comprehension, and patience this achievement would not have been possible.

I would also like to thank:

Professors Mauricio Toro and Andrés Gómez for their help in the preparation, analysis and review of this document, and in general, in the development of this research.

Reviewers for their valuable comments and contributions to the improvement of this document.

Diego Chalarca and Ricardo Román for their assistance with the model and all their advices and suggestions.

Universidad Nacional de Colombia for be literally as my second home all these years, the academic and personal experiences lived here, and the funding received to develop this work. This research was also supported by funding from COLCIENCIAS through the program “Young researchers”. I am deeply grateful for the support from both institutions.

EPM and the project “Estudio de la problemática ambiental de tres embalses de Empresas Públicas de Medellín E.S.P para la gestión integral y adecuada del recurso hídrico” for allowing me to use the field data collected in the project to develop this research.

Centre for Water Research from the University of Western Australia for allowing me to use the model ELCOM-CAEDYM.

M2-215 for all their help in the stressful moments, their comments, laughs, and fun moments have made my time at the master so memorable.

Abstract

The mechanisms of thin phytoplankton layers development were investigated in the tropical La Fe reservoir in terms of the balance between convergence processes acting to thin the layers and turbulent diffusion acting to dissipate them. Our approach included the analysis of field data collected in a field campaign during September 2012, the calibration of the hydrodynamic and ecological model ELCOM-CAEDYM, and the application of a scaling analysis in order to understand and define the processes involved in the formation, maintenance and dissipation of the observed thin layers in the reservoir. Based on the scaling analysis applied to identify the mechanisms participating in the layering process, we defined in situ growth as the primarily mechanism involved in the formation of the layers. The influx of nutrients due to horizontal intrusions and vertical turbulent fluxes influenced this mechanism. Other analyzed mechanisms were convergent swimming and buoyancy of phytoplankton cells. The stratification of the water column together with the dissipation rates responsible to the turbulence around the layers defined local region with favorable conditions to the development of thin layers. Further studies are needed in order to characterize more precisely the mechanisms involved in the development of phytoplankton layers in this reservoir and other environments.

Keywords: Thin layers · Phytoplankton · Distribution · Mechanisms · Reservoir · *Chlorophyll a* · Water column

Resumen

Los mecanismos responsables de la formación de capas delgadas de fitoplancton en el embalse tropical La Fe fueron investigados en términos del balance entre los procesos de convergencia que actúan comprimiendo las capas y los procesos difusivos que actúan disipándolas. Nuestro planteamiento incluye el análisis de datos de campo medidos en una campaña de campo realizada en Septiembre de 2012, la calibración del modelo hidrodinámico y ecológico ELCOM-CAEDYM y la parametrización de los mecanismos analizados con el fin de entender y definir los procesos involucrados en la formación, permanencia y disipación de las capas de fitoplancton observadas en el embalse. Basados en la parametrización desarrollada para identificar los mecanismos participantes en la formación de las capas de fitoplancton, definimos el crecimiento in situ de las células de fitoplancton como el principal mecanismo responsable de la formación de las capas. El flujo de nutrientes debido a la intrusión horizontal y a los flujos turbulentos en la vertical influenció este mecanismo. Los otros mecanismos analizados están relacionados con el desplazamiento y la boyancia de las células de fitoplancton en la columna de agua. La estratificación de la columna de agua junto con las velocidades de disipación responsables de la turbulencia alrededor de las capas definieron regiones locales con condiciones favorables para el desarrollo de las capas delgadas de fitoplancton. Se necesitan más estudios para caracterizar más precisamente los mecanismos que participan en el desarrollo de las capas de fitoplancton en este embalse y en otros escenarios.

Palabras clave: Capas delgadas · Fitoplancton · Distribución · Mecanismos · Embalse · *Clorofila a* · Columna de agua

Contents

List of figures

List of tables

Introduction

The variations of phytoplankton concentration along the water column are common and recognized as a recurrent feature in coastal and oceanic environments, and inland waters for over years (Alldredge et al., 2002; Dekshenieks et al., 2001; McManus et al., 2003; Vidal, Moreno-Ostos, Escot, Quesada, & Rueda, 2010; Vidal, Rigosi, Hoyer, Escot, & Rueda, 2014; Wang & Goodman, 2009). Depending on different gradients in the water column (temperature, irradiance, velocities, and nutrients) and their intensity, phytoplankton can accumulate at different depths forming layers of varying vertical extent (George, 1993; Huisman, Van Oostveen, & Weissing, 1999; Serra, Vidal, Casamitjana, Soler, & Colomer, 2007). Particularly, accumulations of cells may form thin layers with higher concentration of phytoplankton, i.e. regions within the water column with intense biological and chemical processes and interactions (McManus et al., 2008; Sevadjian, McManus, & Pawlak, 2010). Such structures have different dynamics and behavior from phytoplankton cells distributed throughout the water mass (Rines, Donaghay, Dekshenieks, Sullivan, & Twardowski, 2002; Vidal et al., 2010). These layers may be formed not only by phytoplankton, but also an aggregation of a wide variety of organisms such as zooplankton and marine snow, as well as viruses and bacteria (Alldredge et al., 2002; McManus et al., 2003; Rines et al., 2002; Sevadjian et al., 2010).

Phytoplankton distributions are often heterogeneous in space and time. Phytoplankton patches may link large scale processes and microscale interactions, ranging scales from kilometers to centimeters (Mitchell, Yamazaki, Seuront, Wolk, & Li, 2008). At large scales, distributions are driven by enhancing growth rates due to processes such as nutrient upwelling and front formation (Lévy, 2008). At small scales, the interaction of phytoplankton with chemical and physical gradients originates the heterogeneity at the water column influencing trophic processes and changes into the food web (Durham & Stocker, 2012; Prairie, Franks, Jaffe, Doubell, & Yamazaki, 2011). In addition, the time scale must be taken into account to define the characteristics and dynamics of thin layers (Prairie et al., 2011), since the effects on the ecosystem in which they occur depend on their duration. Thereby, layers that persist for days to weeks will have more effects than temporary layers (Birch, Young, & Franks, 2008). The extent to which similar conditions remains depend mainly on wind forcing, on the geometry of the water body, and on the phytoplankton community (Vidal et al., 2014).

In general, phytoplankton layers are generated in response to a balance between convergence processes such as growth, regulated buoyancy, vertical migration (Reynolds, 1984; McManus et al., 2003), advective transport (George & Edwards, 1976; George & Heaney, 1978), and

divergence process such as turbulent mixing (Serra et al., 2007; Steinbuck, Stacey, McManus, Cheriton, & Ryan, 2009). These processes change over time, so phytoplankton layers are expected to exhibit a variable behavior (Cloern, Alpine, Cole, & Heller, 1992). Considering physical processes from large-scales (hydrography changes) to small-scales (turbulent mixing) and biological processes for the phytoplankton species in the layers may contribute to discern which mechanisms participate in the development of the layers (McManus et al., 2003). Physical processes acting in large-scales influence phytoplankton distribution due to the changes generated, for example, in the pycnocline. At small scales, layers are developed under stable conditions of the water column where turbulence is low to disperse the layers (Dekshenieks et al., 2001; McManus et al., 2003; McManus et al., 2005). Phytoplankton characteristics such as growth rates, buoyancy and swimming velocities can even superimpose on the physical processes affecting phytoplankton distributions. Thereby, the combination of these biological species-specific processes along with physical processes define the spatio-temporal distribution of thin layers in the water masses (McManus et al., 2003).

Taking into account that the combination of processes related with the formation, maintenance and dissipation of thin phytoplankton layers depend on the particular characteristics and conditions of each layer (McManus et al., 2003), a multidisciplinary approach with measurements at different scales is needed in order to understand layers dynamics and the consequences of these structures over the entire environment in which they occur (Menden-Deuer, 2008).

The overall objective of this research focuses on the analysis of different mechanisms responsible for the development of thin phytoplankton layers, based on the balance between convergence processes forming the layers and the divergence processes that diffuse them. This document is divided in six chapters. The first chapter describes the theoretical framework including definitions, characteristics and criteria for the identification of thin layers. A description of the convergence-diffusion balance and the mechanisms of layer formation, maintenance and dissipation are also presented in this section. This chapter is followed by the motivation behind this study and the objectives defined. Next chapter presents the methods implemented through this research and the following one presents the results and their respective discussion. We close with the chapter of conclusions obtained with this research, and the chapter of recommendations and future work. In this context, this study contributes to knowledge, as an approximation, to the factors and mechanisms that drive phytoplankton formation, maintenance and dissipation in a tropical reservoir.

The results of this research must be taken as an approximation of the real ones due to the mechanisms involved in the development of the observed thin layers were not measure directly, instead, those were estimated numerically from the observed distributions of thin phytoplankton layers and an hydrodynamic and ecological model. It was observed that the coupling between physical, chemical and biological measurements with a numerical model may provide insights into the responses of phytoplankton to the changes in the water column and help to develop most appropriate strategies to manage and control water quality in reservoirs.

1. Theoretical framework

1.1 Thin phytoplankton layers

Thin phytoplankton layers are aggregations of large numbers of photosynthetic organisms within a small depth interval (Durham & Stocker, 2012). These layers exhibit optical, acoustical, physical, chemical, and biological characteristics that are different from the characteristics presented by other distributions of phytoplankton cells in the water column (Cowles, Desiderio, & Carr, 1998; McManus et al., 2003; McManus et al., 2005, 2008). This kind of layers was first reported by Gessner (1948) and then by Lorenzen (1967) using in vivo fluorescence as technique to detect *chlorophyll* maxima. A detailed description of *chlorophyll* profiles was made by Strickland (1968), followed by Derenbach, Astheimer, Hansen, & Leach (1979). Since then, phytoplankton layers have been observed in a variety of environments in vertical scales of a few meters to horizontal extent of kilometers (Anneville & Leboulanger, 2001; Cheriton, McManus, Stacey, & Steinbuck, 2009; Mitchell et al., 2008; E. Moreno-Ostos, Cruz-Pizarro, Basanta-Alvés, Escot, & George, 2006; Velo-Suárez, Fernand, Gentien, & Reguera, 2010).

1.1.1 Characteristics

There are different kinds of phytoplankton aggregations within the water column including thin layers, deep *chlorophyll* maximum (DCM) and ephemeral small-scale patches. Thin layers are distinct from DCM by their fine vertical scales. Thin layers have thicknesses of a fraction of a meter to a few meters, much stronger vertical concentration gradients (Dekshenieks et al., 2001), and these layers can even have concentrations of phytoplankton cells much greater than the background concentrations (Durham & Stocker, 2012). On the other hand, DCM presents typically a less intense increase in *chlorophyll* concentrations (McManus et al., 2008), thickness of tens of meters, and weak vertical gradients of *chlorophyll* in the water column (Cullen, 1982). In another way, thin layers are distinguished from ephemeral small-scale patches by both shape and persistence time (Durham & Stocker, 2012). Thin layers have aspect ratios (horizontal to vertical extent) of the order of 1,000 (Moline et al., 2010) and last hours to weeks, in contrast to small-scale patches with aspect ratios closer to unity and lifetimes of some minutes (Mitchell et al., 2008).

Thin phytoplankton layers have usually been identified as spikes in vertical profiles of fluorescence in the water column (Birch et al., 2008; Durham & Stocker, 2012). These spikes are

often many times the background concentration with tens of centimeters to a few meters thick, extend horizontally for kilometers, and persist for hours to days (Dekshenieks et al., 2001; McManus et al., 2003; Moline et al., 2010). In general, these layers often occur in regions of strong vertical density gradients and low turbulent mixing (Dekshenieks et al., 2001).

Thin phytoplankton layers tend to occur within the euphotic zone during the daytime, but they can also occur at nighttime some meters below the water surface (Wang & Goodman, 2009). This behavior is driven by the vertical gradient of light and nutrients in the water column and the vertical migration characteristics of each species of phytoplankton. Thus, phytoplankton organisms can stay in the well-lit surface waters during the day (Ryan, McManus, & Sullivan, 2010; Sullivan, Donaghay, & Rines, 2010) and move deeper at night where higher concentrations of nutrients are available and predation risks are reduced (Bollens, Rollwagen-Bollens, Quenette, & Bochdansky, 2011).

Many thin layers are formed by motile phytoplankton species (Bjornsen & Nielsen, 1991; Steinbuck et al., 2009; Sullivan, Donaghay, et al., 2010; Townsend, Bennett, & Thomas, 2005), but also thin layers of nonmotile species, such as diatoms, have been observed (Alldredge et al., 2002; Stacey, McManus, & Steinbuck, 2007; Sullivan, Donaghay, et al., 2010). Furthermore, depending on the buoyant characteristics of the phytoplankton cells, they will tend to accumulate near the surface (positively buoyant), at the bottom of the mixing layer (negatively buoyant), or be randomly distributed in the water column (neutrally buoyant) (Vidal et al., 2014).

1.1.2 Criteria for identifying thin layers

The work published by Dekshenieks et al. (2001) was the first study that define criteria to identify thin layers. However, universal criteria to identify thin layers from others forms of phytoplankton aggregations do not exist due to the diversity of organisms, instrumentation, and environmental conditions in each location where these structures are observed (Sullivan, McManus, et al., 2010). Some common criteria have been established based on the thickness and concentration of phytoplankton cells in the layers (Dekshenieks et al., 2001; Sullivan, McManus, et al., 2010):

a) The aggregation must be identifiable in two or more subsequent vertical profiles. This helps to preserve the spatial coherence of the measurement.

b) The vertical extent of the layer must be no more than 5 m thick. This thickness was defined due to it is finer than the scale often used in the measurements with bottles and nets. The statistics of multiple studies on thin layers have shown that a 3 m cutoff is more adequate (Ryan et al., 2010).

c) The maximum concentration must be at least three times the local background concentration. This criterion eliminates from the observations ephemeral aggregations.

Thresholds differ among studies, and some studies use additional criteria (Durham & Stocker, 2012).

1.2 Convergence–diffusion balance

Based on the scaling framework developed by Stacey et al. (2007) describing layering process as the result of the balance between convergence and divergence processes, we evaluate which of the considered mechanisms participate in the formation and maintenance of the observed thin phytoplankton layers taking into account the effect of turbulent diffusion.

Defining the characteristic length scale for the vertical thickness of the layer as l and the net rate of change of the layer thickness as

$$\left(\frac{\partial l}{\partial t}\right)_{net} = \left(\frac{\partial l}{\partial t}\right)_{convergence} + \left(\frac{\partial l}{\partial t}\right)_{turb} \quad (1)$$

where the first term on the right side includes the different convergent mechanisms acting to thin the layer (negative), and the second term on the right side refers to the diffusive processes acting to dissipate the layer or at least maintain the layer thickness (positive). During the layer formation, convergence processes are more important than the processes trying to broaden the layer, leading to reduce layer thickness (the net rate of change of the layer thickness would be negative). In contrast, during the layer dissipation period the opposite occurs due to the diffusive processes acting to broaden the layer are stronger than other processes (the net rate of change of the layer thickness would be positive). An equilibrium condition is achieved when the convergence processes are balanced by the diffusive processes. Thus, the equilibrium condition for layer maintenance is given by

$$\left(\frac{\partial l}{\partial t}\right)_{convergence} + \left(\frac{\partial l}{\partial t}\right)_{turb} = 0 \quad (2)$$

Considering turbulent diffusion acting in the cross-layer direction (assuming isotropic turbulence), the rate of change of layer thickness as a result of turbulent diffusion is given by (see, e.g., Fischer, List, Koh, Imberger, & Brooks (1979))

$$\left(\frac{\partial l^2}{\partial t}\right)_{turb} = 2k_z \quad (3)$$

where k_z is the vertical turbulent diffusion coefficient. This equation reduces to

$$\left(\frac{\partial l}{\partial t}\right)_{turb} = \frac{k_z}{l} \quad (4)$$

Thereby, the rate of change of layer thickness as a result of turbulent diffusion decreases with layer thickness. Thus, the equilibrium condition takes the form

$$\left(\frac{\partial l}{\partial t}\right)_{convergence} + \frac{k_z}{l} = 0 \quad (5)$$

This equilibrium condition allows layers to persist through the balance between convergence and diffusion processes. Others diffusion processes may be acting to disperse the layers (e.g., contraction and expansion of isopycnals and undirected swimming), but in this scaling analysis only turbulence diffusion is considered as a mechanism responsible to dissipate the observed layers.

These results define a scaling approach to the change of layer thickness based on convergence processes acting to thin the layer and diffusive processes acting to broaden it. These scaling results are applied to different convergent mechanisms to differentiate among them.

1.3 Mechanisms

Owing to the several factors associated with the development of thin phytoplankton layers, it is unlikely that a single mechanism governs all observed layers (Stacey et al., 2007; Prairie, Franks, & Jaffe, 2010). Different convergent mechanisms have been suggested to explain the formation and maintenance of layers of high phytoplankton biomass in the pycnocline considering the homogenizing effect of turbulent diffusion. In this context, the challenge lies in connecting scaling approach with field observations to define the mechanisms, processes, and factors underlying layers development.

1.3.1 Straining

Any process that generates horizontal distribution of water properties may form layers of those properties in the presence of vertical shear (Birch et al., 2008). This is the result of differential advection, whereby a patch is transported at different flow velocities until it is transformed into a thin layer (see Figure 1-1) (Durham & Stocker, 2012). This mechanism was initially proposed by Eckart (1948) to explain field observations of temperature and then extended to phytoplankton layers (Franks, 1995; Osborn, 1998).

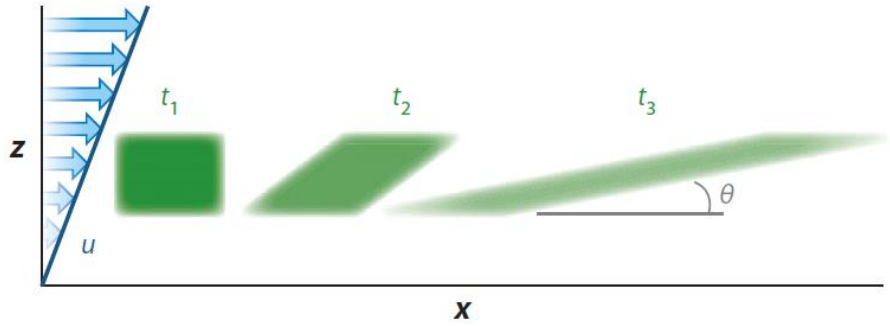

Figure 1-1 Straining transforms a patch at time t_1 into a thin layer by progressively tilting it. Figure taken from (Durham & Stocker, 2012).

Initially, the dynamic of the layer is more influenced by straining than turbulent diffusion. Thereby the layer thickness will monotonically approach zero and, unlike other mechanisms, the phytoplankton concentration in the layer might be the same as straining cannot increase the local concentration of phytoplankton by itself (Durham & Stocker, 2012). However, its thickness decreases until the turbulent diffusion becomes stronger to broaden the layer, reducing phytoplankton concentration and increasing the layer thickness, thus placing a limitation on the lifetime and intensity of strained layers (Durham & Stocker, 2012).

Based on the scaling analysis of Stacey et al. (2007) and the mathematical treatment of Steinbuck et al. (2010), the rate of change of layer thickness due to straining scales as

$$\left(\frac{\partial l}{\partial t}\right)_{straining} \sim -U\frac{l}{l_x} \sim \frac{l^2}{l_x}\frac{\partial u}{\partial z} \quad (6)$$

This scaling relationship defines the velocity in terms of the layer thickness and vertical shear, $U \sim l\left(\frac{\partial u}{\partial z}\right)$, and where l_x is the horizontal length scale of the initial phytoplankton patch (Steinbuck et al., 2010). In the equilibrium, the straining-diffusion balance takes the form

$$-\left(\frac{\partial l}{\partial t}\right)_{straining} \sim \left(\frac{\partial l}{\partial t}\right)_{turb} \quad (7)$$

The horizontal length scale of the initial phytoplankton patch, with constant shear and diffusivity, can be estimated as

$$lx \sim \frac{l^3\left(\frac{\partial u}{\partial z}\right)}{k_z} \quad (8)$$

1.3.2 Convergent swimming

For both zooplankton and phytoplankton species, motility is normally considered as one of the mechanism responsible for the formation and maintenance of thin layers (Genin, Jaffe, Reef,

Richter, & Franks, 2005; Rines et al., 2002). Many factors including a specific light intensity and nutrients concentrations can contribute to the formation of phytoplankton layers at particular depths by convergent swimming (see Figure 1-2) (Durham & Stocker, 2012).

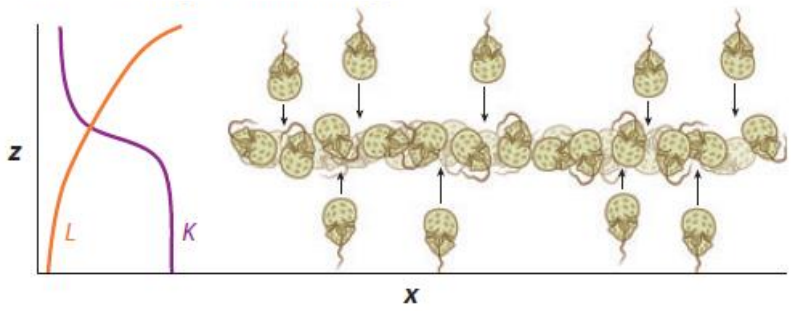

Figure 1-2 Aggregation of cells in a layer at depth with favorable conditions (e.g., a specific light intensity (L) and nutrient concentration (K)). Figure taken from (Durham & Stocker, 2012).

Convergent swimming as the mechanism responsible of layering formation has been modeled assuming that cells aggregate at a particular depth. Stacey et al. (2007) proposed a model to determine the rate of convergence due to species motility in which it assumes that cells swim vertically at a constant velocity (w_s) and oriented toward a target depth (z_o) from both above and below that depth. If $W(z)$ corresponds to the vertical swimming velocity of the organism as a function of depth (with z and W positive downward), the model developed by Stacey et al. (2007) is given by

$$W(z) = -w_s \text{ for } z > z_o \text{ and } W(z) = w_s \text{ for } z < z_o \quad (9)$$

Assumptions considered in this model are justified in terms of the relative displacement and stronger gradients observed vertically than horizontally in properties such as light, nutrients, and temperature (Franks, 1992).

In terms of the vertical swim velocity of cells in and around the layer, the rate of change of layer thickness due to convergent swimming is given by

$$\left(\frac{\partial l}{\partial t}\right)_{swimming} \sim -w_s \quad (10)$$

Thus, the swimming-diffusion balance takes the form

$$-\left(\frac{\partial l}{\partial t}\right)_{swimming} \sim \left(\frac{\partial l}{\partial t}\right)_{turb} \quad (11)$$

And the vertical swim velocity required to maintain the layer scales as

$$w_{balance} \sim \frac{k_z}{l} \quad (12)$$

1.3.3 Buoyancy

Particle buoyancy is other mechanism frequently observed in the formation and maintenance of layers on pycnoclines (Franks, 1992). Nonmotile phytoplankton species can also control their vertical position in the water column by regulating their buoyancy (i.e., the difference between their density (ρ_c) and the water around (ρ_o)), see Figure 1-3. For this, they use mechanisms such as gas vacuoles, carbohydrate ballasting, and active replacement of ions in the internal sap (Durham & Stocker, 2012).

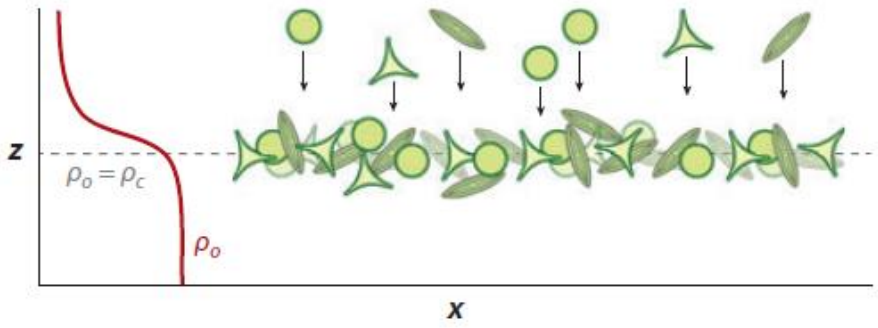

Figure 1-3 Nonmotile cells can sink (if heavier), rise (if lighter), or accumulate at their depth of neutral buoyancy (dotted line), generally at pycnoclines. Figure taken from (Durham & Stocker, 2012).

Considering a phytoplankton cell of density ρ_c retained at an isopycnal of density ρ_o (i.e., $\rho_o = \rho_c$). If the cell is moved from its equilibrium position, a buoyancy-induced force acts on the particle returning it to its equilibrium depth (Stacey et al., 2007). For low Reynolds numbers and as a first approximation, Stokes' law can be used to estimate a settling velocity at which a phytoplankton cell will displace back toward its equilibrium depth. This velocity can be then used to define a scaling relationship to the rate of change of layer thickness due to the effects of buoyancy on phytoplankton cells:

$$V_{settle} = \left(\frac{\partial l}{\partial t}\right)_{buoyancy} = -\frac{\Delta\rho g D^2}{\rho_o 18\mu} \quad (13)$$

where $\Delta\rho$ is the difference between the cell density and water density, D is the cell diameter (assuming a spherical shape), g is the gravitational acceleration, and μ is the molecular viscosity of water (Stacey et al., 2007).

We based our analysis on a cell in equilibrium at the center of a linear density profile ($z = z_o$), where the density difference can be associated to the position of the cell by

$$\frac{\Delta\rho}{\rho_o} g = -\frac{g}{\rho_o}\frac{\partial\rho}{\partial z}(z - z_o) = N^2(z - z_o) \quad (14)$$

where N^2 is the squared buoyancy frequency defined as

$$N^2 = -\frac{g}{\rho_o}\frac{\partial \rho}{\partial z} \quad (15)$$

Thus, the rate of change of layer thickness takes the form

$$\left(\frac{\partial l}{\partial t}\right)_{buoyancy} = -\frac{N^2 D^2}{18\mu}(z - z_o) \quad (16)$$

Scaling $(z - z_o)$ as the layer thickness leads to

$$\left(\frac{\partial l}{\partial t}\right)_{buoyancy} = -\frac{N^2 D^2}{18\mu} l \quad (17)$$

Now, the settling-diffusion balance takes the form

$$-\left(\frac{\partial l}{\partial t}\right)_{buoyancy} \sim \left(\frac{\partial l}{\partial t}\right)_{turb} \quad (18)$$

Solving for the phytoplankton cell diameter required to counteract turbulent diffusion (Steinbuck et al., 2010)

$$D_{balance} \sim \sqrt{\frac{18\mu k_z}{l^2 N^2}} \quad (19)$$

1.3.4 In situ growth

The formation of layers of locally enhanced biomass at mid-depth may occur as the growth response of organisms to non limited conditions of light intensity and nutrients (see Figure 1-4) or to the availability of nutrients over a specific range of depths (Durham & Stocker, 2012). Here, we have considered the formation of layers due to in-situ growth based on the influx of nutrients in both ways: horizontal intrusions and vertical turbulent fluxes.

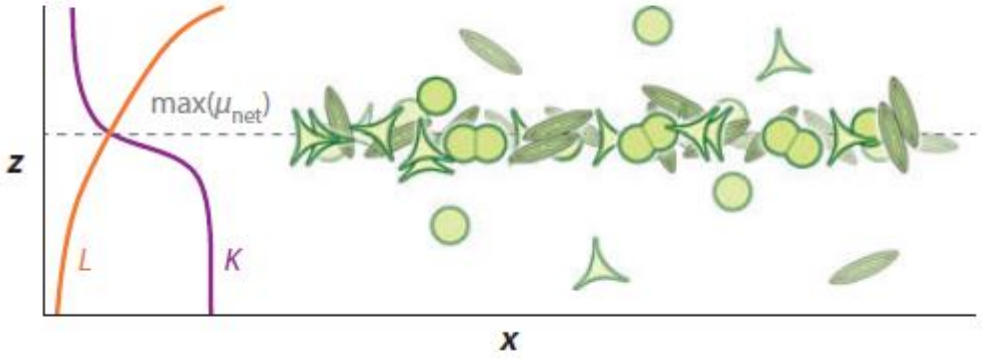

Figure 1-4 Layer formation due to in situ growth at a specific depth with favorable conditions (e.g., light intensity (L) and nutrient concentration (K)). The depth of maximal growth rate is denoted by a dotted line. Figure taken from (Durham & Stocker, 2012).

Intrusions can produce layers of phytoplankton directly through the transport of phytoplankton cells into adjacent waters or alternatively by the advective transport of nutrients-rich waters that then will enhance growth rates at local-depth (Durham & Stocker, 2012). In all cases, intrusions play a key role in supporting phytoplankton layers. Here, we evaluate whether intruding waters could have carried nutrients that then enhanced growth rates of phytoplankton. The increase in *chlorophyll a* concentration caused by growth (ΔC_{growth}) can be estimated from a discrete form of the growth term in the advection-diffusion equation (Steinbuck et al., 2010)

$$\Delta C_{growth} = \mu_{net} C_b t_{prop} \quad (20)$$

where μ_{net} is the net production rate of *chlorophyll a* (growth minus mortality), C_b is the background *chlorophyll a* concentration, and t_{prop} is the time scale of intrusion propagation (Fischer et al., 1979) estimated as

$$t_{prop} \sim \frac{L^2}{2k_H} \quad (21)$$

where L is the characteristic length scale of the patch and k_H is the horizontal dispersion coefficient. This time scale implies an equilibrium flow where growth dominates over advection and diffusion processes due to its shortest time scale (Imberger, 1977; Imberger et al., 1983).

The horizontal dispersion coefficient may be expressed by

$$k_H = \alpha L^{\beta} \quad (22)$$

with $\alpha = 3.2x10^{-4}$ and $\beta = 1.1$ (Lawrence, Ashley, Yonemitsu, & Ellis, 1995). These parameters incorporate the effects of factors such as surface heat fluxes, wind speed, direction, turbulence levels, and the inevitable measurement errors. Values obtained with this equation have 95 percent probability of being accurate within a factor of approximately 2.5 over length scales ranging from 10 m to > 100 km (Lawrence et al., 1995).

Now, comparing ΔC_{growth} with the observed *chlorophyll a* anomaly of the layers (ΔC_{obs}) defined as the difference between the concentration at the maximum peak minus the background concentration (C_b) of the layer (Steinbuck et al., 2010), we establish the viability of layer formation due to in-layer growth.

A second possible mechanism for stimulating growth in layers is given by vertical turbulent fluxes of nutrients (Steinbuck et al., 2010)

$$F_N = -k_z \left[\frac{\partial C_N}{\partial z}\right] \quad (23)$$

where C_N is the nutrient concentration.

The timescale required to supply the nutrients needed to support in-layer growth of phytoplankton cells (Steinbuck et al., 2010) can be defined as

$$T_{supply} = \frac{\Delta N_{anom}}{F_N} \quad (24)$$

where ΔN_{anom} is the anomaly in the in-layer, vertically-integrated nutrients (nitrate or phosphate) required to support the observed *chlorophyll a* layers. This timescale (T_{supply}) assumes that the nutrients entering the layer are completely taken up by the phytoplankton cells (Steinbuck et al., 2010).

1.3.5 Other mechanisms

In addition, other physical and/or biological processes may play a role in thin layer formation not only forming the layer, but also contributing to its maintenance. These processes include for example gyrotactic trapping, reproduction, the increase in local viscosity, and differential grazing. Gyrotactic trapping is a mechanism based on the movement of motile phytoplankton into a region where flow induces tumbling of the cells, trapping them at depth in the form of a thin layer (Durham, Kessler, & Stocker, 2009; Durham & Stocker, 2012). Higher concentrations of phytoplankton could lead to increase reproduction rates, this may be important to some kinds of thin layers especially those formed during blooms (Nielsen, Kiørboe, & Bjørnsen, 1990). Phytoplankton cells can also contribute to the maintenance of the layer increasing the local viscosity of the surrounding waters and therefore reducing the turbulent diffusion acting on the layer (Jenkinson & Biddanda, 1995). Alternatively, the inhibition of potential predators may help to preserve the phytoplankton layers. In this case, zooplankton may avoid certain kinds of phytoplankton layers (e.g., layers formed by toxic species) helping to maintain those layers (Fiedler, 1982; Bjornsen & Nielsen, 1991). It is likely that several mechanisms are operating simultaneously at any given time. The relative contribution of any mechanism will depend on the local environment conditions and the planktonic community present in the water column (Franks, 1995).

1.4 Maintenance

The mixing environment can be characterized in terms of the stabilizing influence of the density gradient and the disturbing effect of velocity shear. Both parameters provide a framework to understand which conditions are favorable for layer persistence or not (Cowles et al., 1998). In general, stratification contributes to the formation and maintenance of phytoplankton layers in two ways: facilitating accumulation of the sinking cells that reach neutral buoyancy at a pycnocline and reducing vertical turbulent mixing in the water column (Durham & Stocker, 2012). On the other hand, shear can favor layer formation via mechanisms such as straining or gyrotactic trapping, but it can also generate instabilities and turbulence in the water column diffusing layers.

The net stability of the water column is determined by the gradient Richardson number (Ri), given by the ratio of the squared buoyancy frequency (N^2), and the squared shear (S^2)

$$Ri = \frac{N^2}{S^2} \quad (25)$$

where the squared vertical shear is defined, after Itsweire, Osborn, & Stanton (1989), as

$$S^2 = \left(\frac{dU}{dz}\right)^2 + \left(\frac{dV}{dz}\right)^2 \quad (26)$$

where U and V are the components of the horizontal velocities.

Persistent local minima in shear and local maxima in the density gradient create regions of stability that allow thin layers to persist. Conversely, local increments in shear and/or local decrements in the density gradient can dissipate small-scale structure through shear instabilities (Cowles et al., 1998). The critical value of $Ri = 0.25$ has been accepted as a boundary between a stable or unstable water column (Eriksen, 1978; Miles, 1961; Scotti & Corcos, 1972). Thus, when Ri is greater than 0.25 the water column is expected to be stable to shear-instabilities (Miles, 1961) and, in this way, able to support thin layer formation and maintenance (Dekshenieks et al., 2001; McManus et al., 2003).

Moreover, the competition between stratification and turbulent mixing can be assessed through the buoyancy Reynolds number defined as

$$Re_b = \frac{\varepsilon}{\mu N^2} \quad (27)$$

where ε is the turbulent dissipation rate. Based on this number, it has defined that turbulence is in general unaffected by stratification for $Re_b > \sim 100$ (Steinbuck et al., 2009). Stratification significantly affects the turbulence in the range $\sim 15 < Re_b < \sim 100$ (resulting in anisotropies), and dominates turbulence for $Re_b < \sim 15$ (Itsweire, Koseff, Briggs, & Ferziger, 1993; Ivey &

Imberger, 1991). In this last case, turbulence is insufficient to broaden the layer through vertical mixing (Steinbuck et al., 2010).

1.5 Dissipation

To analyze the role of layer divergence on the development of a thin phytoplankton layer, we need to estimate the vertical turbulent diffusion coefficient (k_z). In order to reduce the broad uncertainty associated with this coefficient (Stacey et al., 2007), two methods have been applied to calculate turbulent dissipation rate.

1.5.1 Thorpe scale

We begin with the estimation of the Thorpe scale, also called overturning scale (L_t). This scale was calculated as the root mean square displacement (l_d) of water parcels from their equilibrium vertical position, based on the reordering of the density profile to make it gravitationally stable (Thorpe, 1977). In this sense, we first calculated from each measured and sorted profile of temperature:

$$L_t = \sqrt{{l_d}^2} \quad (28)$$

Assuming that the Thorpe scale is equal to the Ozmidov scale (see, e.g., Gregg, 1987), where the Ozmidov scale (Lo) is estimated as

$$Lo = \left(\frac{\varepsilon}{N^3}\right)^{1/2} \quad (29)$$

the turbulent dissipation rate can be defined as

$$\varepsilon = {L_t}^2 N^3 \quad (30)$$

Based on this estimation of the turbulent dissipation rate and considering a local balance between shear production, dissipation rate, and buoyancy flux, we may estimate the turbulent diffusion coefficient through (Osborn, 1980)

$$k_z = \gamma_{mix} \frac{\varepsilon}{N^2} \quad (31)$$

The value of mixing efficiency (γ_{mix}) is generally at or close to 0.2 (Osborn, 1980). This value depends on turbulence conditions of the medium.

1.5.2 Turbulent fluctuations

An estimation of the dissipation rate based on the turbulent density fluctuations is given by (Itsweire et al., 1993)

$$\varepsilon = (4\sim5)\varphi N^2 C_z \quad (32)$$

where φ is the molecular diffusivity and C_z the vertical Cox number defined as

$$C_z = 3\frac{\overline{\left(\frac{\partial \rho'}{\partial z}\right)^2}}{\left(\frac{\partial \bar{\rho}}{\partial z}\right)^2} \quad (33)$$

where ρ' designates the density fluctuations and $\bar{\rho}$ the density average over 0.1 m vertical bin cells. Bins are defined as the length of the observation windows in which the vertical profile is divided and where the vertical attributes of the profile within each bin are averaged.

2. Motivation

Generally, thin phytoplankton layers extend a few meter in vertical but extend for kilometers horizontally (Dekshenieks et al., 2001; McManus et al., 2003). This characteristic behavior of the layers has implications in many ecological and global processes such as fisheries productivity and climate (Mitchell et al., 2008; Sonntag & Hense, 2011). Accumulation of phytoplankton cells into thin layers may affect many ecological functions in the environment in which they occur, influencing trophic processes such as feeding, reproduction, growth, remineralization, competition and predation by other organisms (Alldredge et al., 2002; Birch et al., 2008; Cowles et al., 1998; McManus et al., 2003). Moreover, thin layers may contain toxic phytoplankton species disrupting grazing, increasing zooplankton and fish mortality (Durham et al., 2009), and enhancing the transfer of toxins to higher trophic levels such as marine mammals and seabirds (McManus et al., 2008).

On the other hand, vertical distribution of phytoplankton relative to the availability of light and nutrients affects not only primary production (Alexander & Imberger, 2008; Ryan, McManus, Paduan, & Chavez, 2008), but also properties of the water column such as surface albedo and surface drag (Holliday, Pieper, Grennlaw, & Dawson, 1998; Holliday et al., 2003; Sonntag & Hense, 2011; Sullivan, Twardowski, Donaghay, & Freeman, 2005; Zaneveld & Pegau, 1998). The concentration of organisms within thin layers is considerably higher than the concentration of organisms distributed immediately above and below the layers (Cheriton et al., 2009). Such dense accumulation of phytoplankton near the surface affects optical properties of the water column altering light penetration and thereby the distributions of heat in the water (Sonntag & Hense, 2011). In addition, these surface mats can disturb the surface wind drag affecting momentum flux and thereby turbulence mixing in the water column (Hutchinson & Webster, 1994).

At the same time, all drivers related with phytoplankton layers are subject to changes over space and temporal scales ranging from hourly to seasonal. Wind direction and magnitude, for example, are subject to diurnal variations due to changes in heating over land and water surface, weather fronts and seasonal variations in atmospheric pressure patterns (Vidal et al., 2010). The mixing environment is also expected to change at different scales (e.g. Fischer et al. (1979); Imberger (1985)). The mixed layer is expected to deepen at night in response to cooling at the surface or strong wind events while stratification of the water column is expected to occur during the day time under strong isolation and weak wind conditions. Aggregations of phytoplankton with

different characteristics can also occur at different times during the season (succession) in response to the thermal stratification of the water column (Vidal et al., 2010).

These drivers changes affect the generation and evolution of vertical and horizontal phytoplankton distributions due to the interaction that exists between physical properties of the water column (i.e. turbulent mixing, thermal structure, advective transport and light irradiance, among others) and the biological characteristics of each phytoplankton group (George & Edwards, 1976; George & Heaney, 1978; Moreno-Ostos et al., 2006; Vidal et al., 2014). For example, as shown by the balance between advective transport induced mainly by wind and the vertical structure of the phytoplankton functional group: positively buoyant species should tend to float near to the surface and concentrate downwind while negatively buoyant species in deep layers should be displaced upwind, and neutrally buoyant cells should be randomly distributed (Vidal et al., 2010). Vertical distribution of phytoplankton can even be linked to horizontal patchiness by physical process such as *conveyor-belt* circulation, in which wind drives movement of currents in opposite directions at different depths in the water column (George & Edwards, 1976; Vidal et al., 2010).

Tropical lakes have different dynamics compared to lakes in middle and high latitudes in part by the absence of seasons. In general, their stratification and mixing patterns are governed by: (1) the small difference between maximum and minimum annual radiation, (2) the relative constant fluxes of heat through the surface during the day as a result of the small diurnal variations of total radiation throughout the year (Lewis, 1987), and (3) the variation in weather conditions such as rainfall (Chaves, Lima, Leitão, Paulino, & Santaella, 2013). In addition, the reduced difference between the temperature at the bottom and the surface affects the stability of the water column and the variation of the epilimnion's thickness (Lewis, 1987). In particular, the distribution of thin layers in these systems has been found to be subject to changes in factors such as light regime in the water column, nutrients and physical process (McManus et al., 2003). Stratification plays a critical role in the transport processes through the water column being a barrier to the transport of nutrients, oxygen, algal cells, heat to the surface and deeper waters (Vuorio, Nuottajärvi, Salonen, & Sarvala, 2003). However, vertical and horizontal phytoplankton aggregations are more intense in stratified water bodies (Moreno Ostos, 2004). Wind direction and magnitude, and changes in temperature may cause the stratification of the water column.

In addition to the particular characteristics and dynamics associated to the geographical position, reservoirs are subject to changes in its hydraulic management. These changes can affect the distribution of phytoplankton patches due to variations in the thermal stability and the mixed layer depth (Cruz-Pizarro, Basanta-Alves, Escot, Moreno-ostos, & George, 2005; Elliott, Escot, Basanta-Alves, & Cruz-Pizarro, 2005; Moreno Ostos, 2004; Toja, Basanta, & Fernández-Ales, 1992). As a result of the changes in the water column the concentration of phytoplankton organisms can be reduced at specific depths, but new thin layers can be generated due to the mixing of layers (Casamitjana, Schladow, & Roget, 1993; Imboden, 1992; Steinberg & Gruhl, 1992). The specific water withdrawal depth, for example, has implications in the amount of

phytoplankton material that is removed from the reservoir affecting or favoring energy generation or water treatment processes depending on the depth in which mainly phytoplankton patches occur (Moreno-Ostos, Cruz-Pizarro, Basanta, & Glen George, 2008).

As we have shown through this section, the appearance of phytoplankton layers has significant implications on ecosystems and water processes, depending layering processes on factors changing over space and time scales. The conditions under which phytoplankton layers develop in tropical environments are even more complex due to the particular characteristics and dynamics of these scenarios. In order to understand the appearance of blooms in water bodies and develop models capable of forecast them and predict their impacts on the ecosystem, first, we need to identify the factors that drive distributions of phytoplankton cells at different spatial and temporal scales (Rines et al., 2002) to then define the characteristics, dynamics and mechanisms governing layering process (Cowles et al., 1998; Gallager, Yamazaki, & Davis, 2004; Serra et al., 2007). A better understanding of thin phytoplankton layers development might help to identify distinct niches and provide insights into the causes for presence, dominance and/or diversity of phytoplankton species in water bodies (Alexander & Imberger, 2008). It might also provide tools for predicting phytoplankton layers events, intensity, and persistence taking into account the biological response of phytoplankton species to the physical environment in which their occur (Dekshenieks et al., 2001; Prairie et al., 2011) as well as the development of strategies to the adequate management and control of water quality in water bodies (Moreno-Ostos et al., 2006; Moreno-Ostos, Cruz-Pizarro, Rueda, Escot, & Basanta-Alvés, 2005; Vidal et al., 2014).

2.1 Objectives

The primary objective of this research is to define the mechanisms responsible for the formation, maintenance and dissipation of thin phytoplankton layers in the Colombian La Fe reservoir. Our approach is: (1) to determine the local variability of external forcing and processes to define the environmental conditions where thin layers develop, (2) to identify the factors that influence phytoplankton thin-layer development relating thin-layer variability to local forcing and processes and, based on these information, (3) to estimate the mechanisms involved in the development of thin phytoplankton layers in order to explain the appearance of these layers in the reservoir.

3. Methods

3.1 Study site

La Fe reservoir is located in the town of El Retiro, Antioquia, Colombia at coordinates 06°06'N, 75°30'W. The water in this reservoir is primarily intended for the supply of drinking water to the community, for recreation (Román-Botero, 2011), and eventual power generation (EPM, 2005). As a result of the expansion in 1974 of the former reservoir named Los Salados, La Fe reservoir is divided in two zones with different characteristics product of the lateral narrowing of the first structure (see Figure 3-1). The bathymetry of this reservoir is also special due to its dam is submerged.

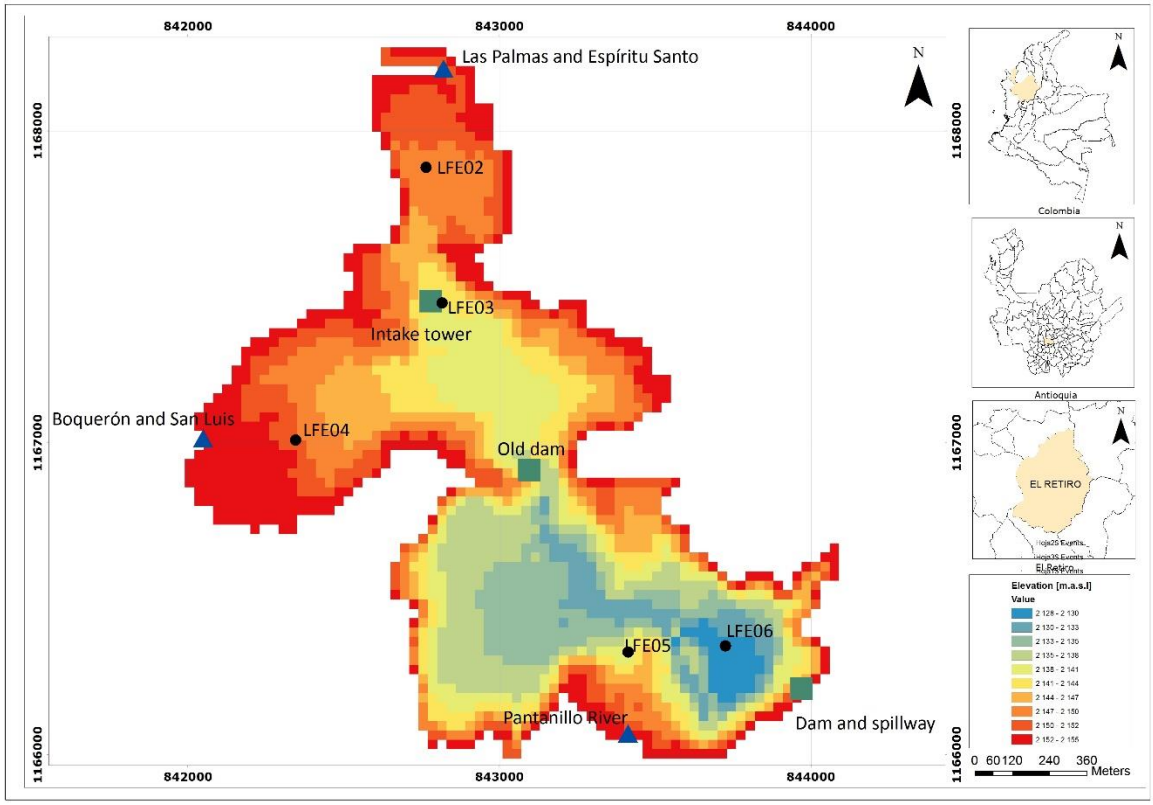

Figure 3-1 Bathymetric map of the La Fe reservoir with inflows location and the measuring stations indicated as LFE02, LFE03, LFE04, LFE05, and LFE06.

The north zone has an area of 0.68 km^2 with mean and maximum depths of 7.0 m and 18.2 m, respectively. The intake tower and the main natural inflows namely Las Palmas and Espíritu Santo at north and Boquerón and San Luis at west are located in this zone (see Figure 3-1). On the other hand, the south zone has an area of 0.65 km^2 with mean and maximum depths of 14.7 m and 26.0 m, respectively. In this zone are located the dam and two inflows of water pumped from the Pantanillo River, one pumped through a surface channel and the other one through a submerged pipeline within the reservoir (Román-Botero, 2011). In this study, we will consider these two inflows just like one due to the lack of detailed data about location, operation, and flow of the submerged pipeline. Thus, we consider a combined inflow of water from the Pantanillo River pumped only through the surface channel. The particular configuration of the reservoir together with its bathymetry make it a special study site.

3.2 Field data

This research was developed with field data collected for the study "Estudio de la problemática ambiental de tres embalses de Empresas Públicas de Medellín E.S.P para la gestión integral y adecuada del recurso hídrico", a joint project developed for Empresas Públicas de Medellín (EPM), by Universidad de Antioquia and Universidad Nacional de Colombia, and which aimed at the understanding of the spatial and temporal evolution of the thermal structure and transport processes in three tropical reservoirs (Riogrande II, La Fe, and Porce II) in Antioquia, Colombia.

Meteorological data include records of solar radiation, air temperature, relative humidity, wind speed and direction, atmospheric pressure, and rainfall collected each 5 minutes with a meteorological station (DAVIS Vantage Pro 2) installed on the intake tower in La Fe reservoir. Water temperature, conductivity, dissolved oxygen, and *chlorophyll a* profiles were recorded using a conductivity–temperature–depth instrument (CTD - Sea-Bird SBE 25) and a fluorescence sensor (bbe FluoroProbe Moldaenke) with up to 8 and 4 measurements per second, respectively, at five stations within the reservoir. In addition, profiles of nutrients (ammonium, nitrate, phosphate, and total phosphorous) were measured in the upper water column at the deepest point of the reservoir using a Van Dorn sample bottle.

Despite we have data of meteorological variables and inflows over a 64-day period from 7th September to 9th November 2012, field data related with the vertical structure of *chlorophyll a* and nutrients both, at the inflows and the reservoir, are limited. In order to consider how these measurements coupled to explain phytoplankton layering processes and the specific relationships these layers have to the major physical-chemical forcing and processes in La Fe reservoir, we focus our analysis only in the field data collected between 25th and 27th of September 2012 in five stations in the reservoir and, specifically, in the deepest point of the reservoir where we have nutrients data. The analyzed stations correspond to stations LFE02, LFE03, LFE04, LFE05, and LFE06 accordingly to the nomenclature used in other studies where these same stations have also been analyzed (Román-Botero, 2011).

3.3 Modeling approach

In this study, measurements of physical variables, *chlorophyll a*, and nutrients along with the three-dimensional hydrodynamic and ecological model ELCOM-CAEDYM are used to investigate the spatial and temporal distribution of thin phytoplankton layers, and the role of physical-chemical-biological drivers and processes in the development of these layers. As in other studies, numerical modeling is used to overcome some of the restrictions imposed by field data, enhancing the spatial and temporal scales of the analysis (Alexander & Imberger, 2008). The modeling approach does not attempt to represent all processes related with the development of the layers, it includes only the most basic ones in order to explain the dynamics of the observed layers. Observed temperature, dissolved oxygen, and *chlorophyll a* profiles collected in 2012 during a field campaign are compared with simulated profiles in order to calibrate the model. The calibration of the model may confirm that the key processes have been represented correctly. In our case, the validation of the model could not be carried out due to the limited data available.

The model ELCOM-CAEDYM was developed by the Centre for Water Research (CWR) of University of Western Australia for simulation of lakes and reservoirs, wetlands, estuaries, and coastal ocean. ELCOM (Estuary, Lake and Coastal Ocean Model) is a numerical model that applies hydrodynamic and thermodynamic equations to simulate the spatial and temporal behavior of stratified water bodies subject to environmental forcing (Hodges & Dallimore, 2012b). The model uses a fixed grid structure to solve the unsteady Reynolds-averaged Navier-Stokes (RANS) and scalar transport equations, subject to boundary forcing and the Boussinesq and hydrostatic approximations, incorporating a mixing model to directly compute vertical turbulent transport (Laval, Hodges, & Imberger, 2003).

Hydrodynamic equations in the model are solved based on the Euler-Lagrange method for advection of momentum with a conjugate-gradient solution for the free-surface elevation (Casulli & Cheng, 1992). Passive and active scalars (i.e. tracers, salinity, and temperature) are advected using a conservative ultimate quickest discretization (Leonard, 1991). Further description and details of the mathematical formulation and solution of the model can be found in (Hodges & Dallimore, 2012a).

The Heat exchange through the water surface is separated into penetrative shortwave radiation and nonpenetrative components of long-wave radiation, sensible heat transfer, and evaporative heat loss. Hence, while nonpenetrative effects are described in terms of standard bulk transfer equations corrected to include the effects of atmospheric stability (Imberger & Patterson, 1989), short-wave radiation penetrates into the water following an exponential decay and an extinction coefficient as described by Beer's Law (Hodges & Dallimore, 2012a).

The transfer of vertical momentum is solved for each water column through a method that is more common to one-dimensional models (e.g. Imberger & Patterson, 1980). The depth of the mixed layer is determined by a balance between the energy produced by wind stirring and

velocity shear, and the energy required to mix a given density gradient in one model time step. The dependency of time-step to the mixing routine is reduced by the model carrying over unused mixing energy to the next time step (Alexander & Imberger, 2008).

On the other hand, CAEDYM (Computational Aquatic Ecosystem DYnamics Model) is a process-based ecological model designed to run independently or coupled with hydrodynamic models (Hipsey, Antenucci, & Hamilton, 2012). The CAEDYM model contains a series of coupled first-order differential equations representing the major biogeochemical processes influencing water quality including primary and secondary production, nutrient and metal cycling, oxygen dynamics, and the movement of sediments (Rigosi, 2010). This model can be used to resolve different species or group specific ecological interactions and processes. In the most complex configuration, it can simulate up to seven phytoplankton groups, five zooplankton groups, fish, macrophytes, and pathogens (Hipsey et al., 2012). Further description and details of the model can be found in (Hipsey et al., 2012).

CAEDYM can resolve at any sub-daily time step algal processes such as diurnal photosynthesis and nocturnal respiration. In general, it is run at the same time interval as the hydrodynamic model ELCOM (Hipsey et al., 2012). Thereby, while ELCOM simulates processes such as wind stresses, surface thermal forcing, inflows, outflows, transport of salt, heat and passive scalars, through coupling with the CAEDYM ecological module, ELCOM is used to simulate three-dimensional transport, interactions and processes of physical, chemical and biological variables (Hodges & Dallimore, 2012b).

3.4 Thin layers development

In order to define the mechanisms of thin phytoplankton layers development, first, we calculated over 0.1 m vertical bin cells the buoyancy frequency, shear, Richardson number, turbulent dissipation rate, turbulent diffusion coefficient, and buoyancy Reynolds number from physical measurements made at the depth range of each layer and the results of the calibrated model. This resolution was chosen in order to average the changes observed in the profiles at small scales.

As we described in the theoretical framework, thin layers are likely the result of various mechanisms operating at any given time. In this study we analyzed convergent swimming, buoyancy, and in situ growth as the mechanisms responsible for the formation of thin phytoplankton layers in La Fe reservoir. Owing to direct measurements of all contributing processes are not practical, and in our case are not possible, drivers of layers have been investigated via indirect techniques (Alexander & Imberger, 2008).

Taking into account that each convergence mechanism produces distinctive layer characteristics and correlations with the biophysical environment, a diagnosis of the processes involved in field observations can be carried out (Durham & Stocker, 2012). In this context and based on the

scaling analysis for these mechanisms, we estimated the following representative parameters: $w_{balance}, D_{balance}, \Delta C_{growth},$ and T_{supply}. Then these parameters were compared to known or inferred values to determine which mechanisms are capable of producing salient features of the layer and to rule out mechanisms with attributes that are incompatible with observations made in the reservoir.

4. Results and discussion

4.1 Field information

4.1.1 Meteorological data

Previous studies in the reservoir have shown the bimodal behavior of rainfall and flows due to the influence of the Inter-Tropical Convergence Zone (ITCZ) in the region (Román-Botero, 2011). Specifically, during the last week of September 2012 in development of the field campaign, the air temperature, short wave radiation, and relative humidity showed the characteristic diurnal behavior of meteorological variables at tropical zones (see Figure 4-1). Air temperature oscillated approximately between 12 and 22 °C with maximum during the day and minimum at night. A similar day–night pattern was shown by the short wave radiation. Otherwise, relative humidity was lowest during the morning and afternoon and reached a maximum value of 1 at night. Long-wave radiation showed a large variation during the day–night cycle. On the other hand, the wind direction was approximately 290–330° around midday, thus blowing from the intake tower to the dam of the reservoir. In the evening the wind reversed to 20–90°, thus blowing from the dam to the main body of the reservoir. Weak winds prevailed, maximum speeds of about 7 m s^{-1} occurring during the midday-afternoon and minimal during the night. A mean rainfall of 16.3 mm occurred at afternoon of 24th of September during 275 minutes. These meteorological data present the typical behavior observed for these variables in previous years during the same period of time.

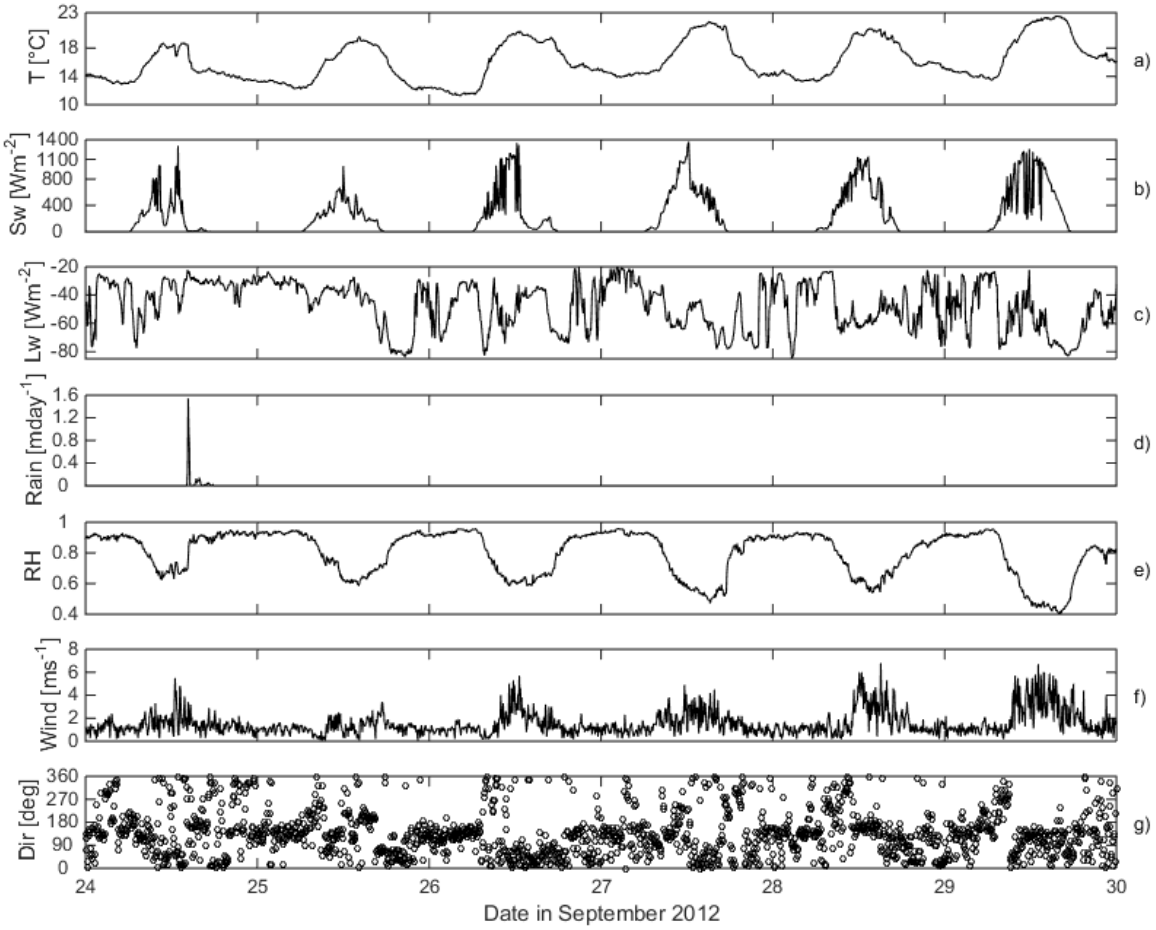

Figure 4-1 Meteorological data: a) air temperature, b) short and c) long wave radiation, d) rain, e) relative humidity, and wind f) magnitude and g) direction.

Inflows rates, during the last week of September, varied from 1.15 to 1.5 $m^3 s^{-1}$ in Las Palmas and Espíritu Santo, and from 0.37 to 0.48 $m^3 s^{-1}$ in Boquerón and San Luis (see Figure 4-2). The total pumped water from the Pantanillo River oscillated from 0 to 6.5 $m^3 s^{-1}$. Outflow varied from 2 to 6 $m^3 s^{-1}$ corresponding to the total water captured by the intake tower. Inflows are greater than the outflow and, consequently, the water level in the reservoir increased during the study period. As observed in the Figure 4-2, the flow of the inflows Las Palmas and Espíritu Santo, and Boquerón and San Luis increased the day 24th of September as a result of the rainfall presented at the afternoon of this day. The water temperature of inflows oscillated both at diurnal and longer time scales in response to meteorological forcing. The range of diurnal temperature oscillations in inflows was up to 5 °C, which is large compared to variations in temperature exhibited at diurnal scales in the reservoir surface. The water temperature of outflow was assumed approximately equal to a value of 17 °C based on field data collected in 2011 under similar conditions in the reservoir.

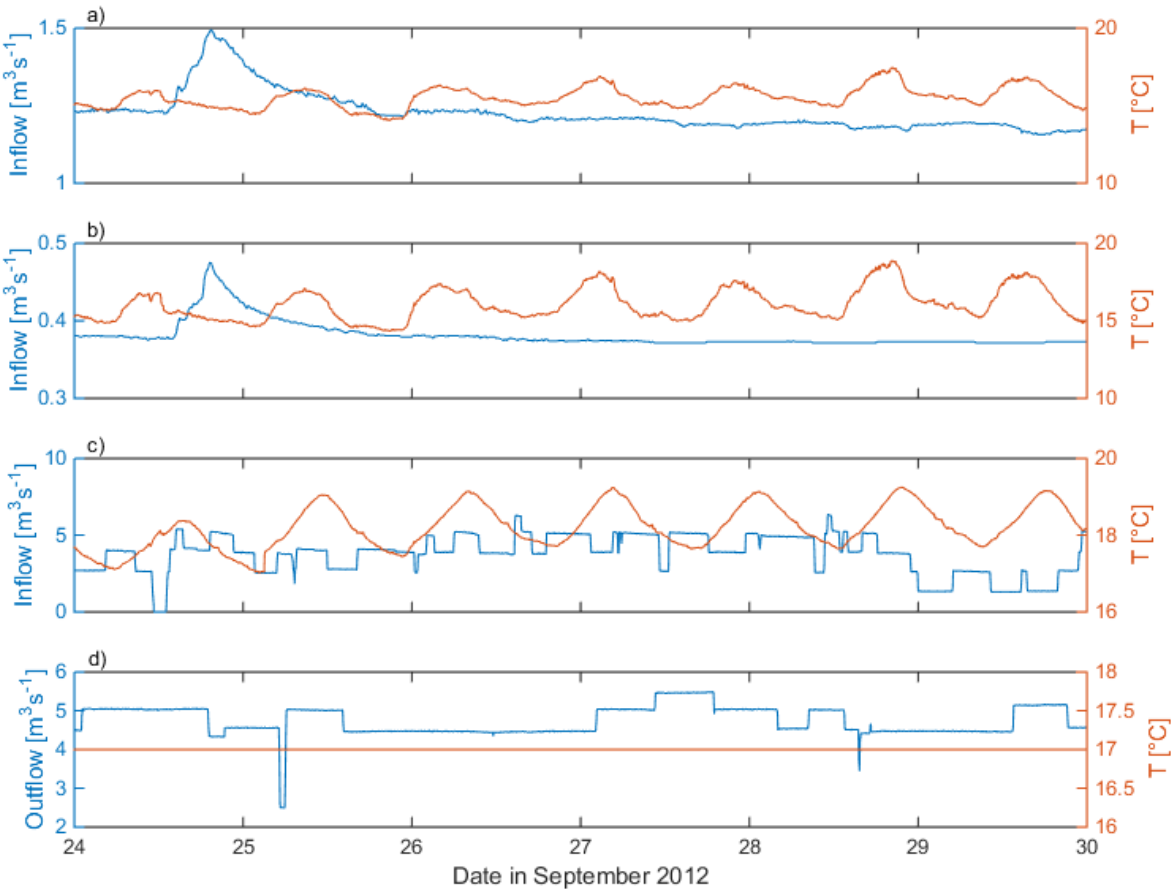

Figure 4-2 Inflows and outflow in the reservoir with their respective temperature: a) Las Palmas and Espíritu Santo, b) Boquerón and San Luis, c) Pantanillo River (total pumped), and d) intake tower (total extracted).

4.1.2 Field observations

Over the study period the temperature, dissolved oxygen, conductivity, and total *chlorophyll a* vertical profiles were different due to the specific characteristics at each measurement station (see Figure 4-3 to Figure 4-7). It was not possible to define clearly the epilimnion, metalimnion and hipolimnion in the temperature profiles due to the weak gradients observed along the water column, as it has been reported by Román-Botero (2011) in a previous research conducted in this same reservoir and other studies (Lewis, 1987; Roldán & Ramírez, 2008).

The main changes in the profiles occurred in the same first meters of the water column. In the upper part of the water column the temperature decreased faster with depth. The maximum oxygen peak depth varied from 2.7 and 3.8 m between profiles. The maximum oxygen concentrations were measured at station LFE04, followed by station LFE06 and then station LFE02, the stations closest to the entrance of flows. The conductivity at stations LFE02 and LFE03 seem to be affected by the intake tower due to the changes in the conductivity profiles coincided

with the depths of the intake gates. Total *chlorophyll a* profiles showed that their maximum peak was positioned within the top 5 m depth with magnitudes from 23.2 to 223.0 µg L^{-1}. Nitrate and phosphate varied from 0.062 to 0.476 mg L^{-1} and 0.004 to 0.014 mg L^{-1}, respectively, with the maximum at the base of the nitracline between 7-10 m depth (see Figure 4-7). At station LFE06, the depth of the maximum *chlorophyll a* peak was allocated top of the nitracline and the phosphocline.

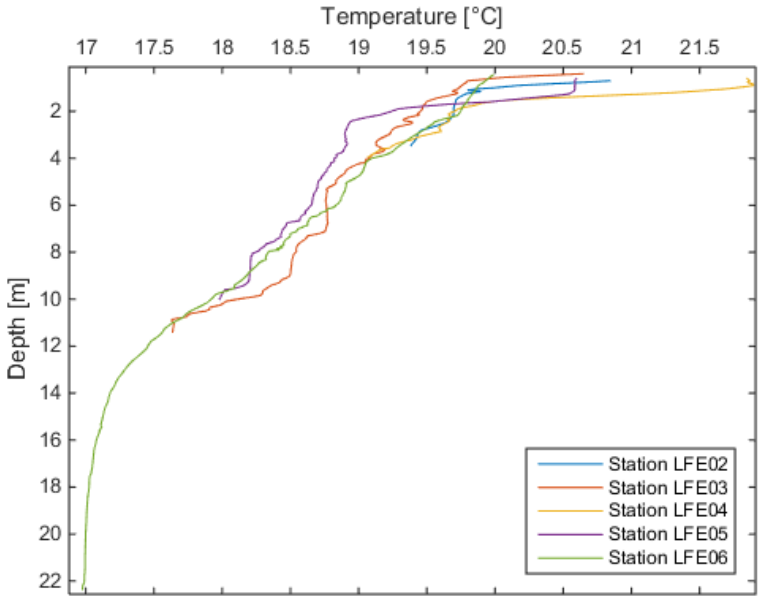

Figure 4-3 Temperature profiles collected between 25th and 27th of September.

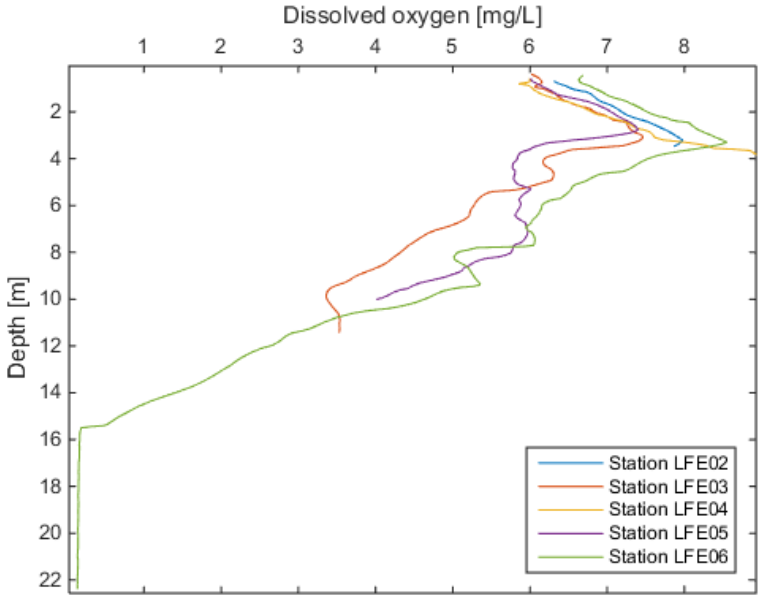

Figure 4-4 Dissolved oxygen profiles collected between 25th and 27th of September.

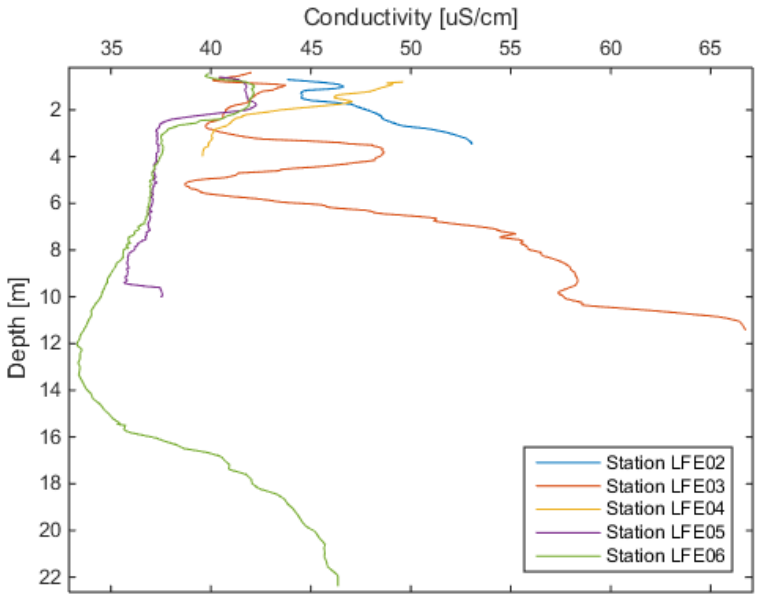

Figure 4-5 Conductivity profiles collected between 25th and 27th of September.

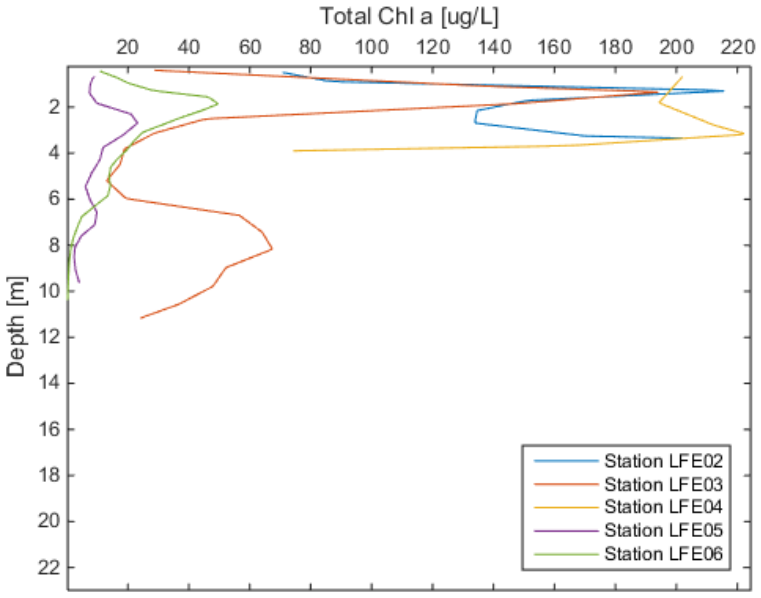

Figure 4-6 Total *chlorophyll a* profiles collected between 25th and 27th of September.

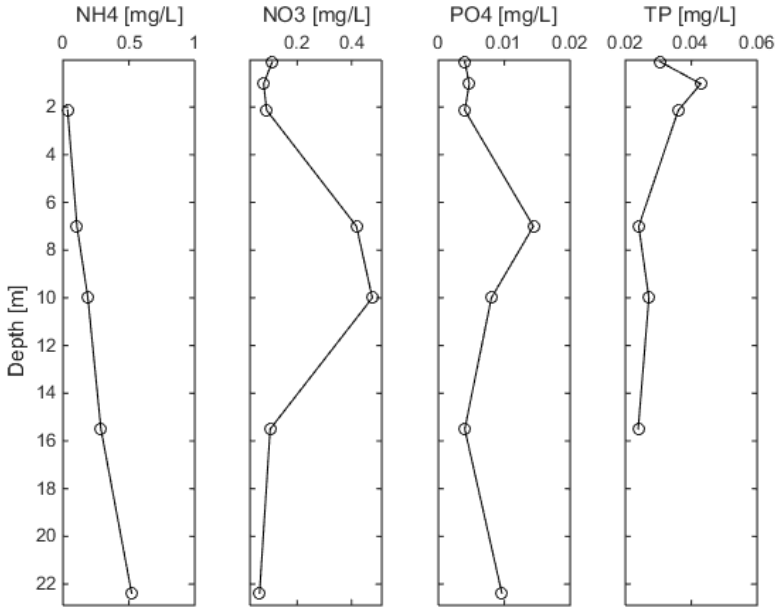

Figure 4-7 Ammonium, nitrate, phosphate, and total phosphorous profiles collected at station LFE06.

4.2 Thin layers identification

Thin phytoplankton layers were identified in each profile by an examination of the fine-scale vertical structure of the *chlorophyll a* concentration profile. The layer thickness was defined as the width of the peak measured at the half concentration of the maximum peak (see Figure 4-8), and the background concentration as the nearest minima surrounding the peak (Prairie et al., 2010). Based on the criteria to identify thin phytoplankton layers mentioned in the theoretical framework and the definitions of layer thickness and background concentration, we identified different thin phytoplankton layers along the reservoir. Attributes of the identified thin phytoplankton layers are presented in Table 4-1. The thickness of the *chlorophyll a* maximum peaks ranged from 1.2 to 3.1 m with its maximum at station LFE04. Maximum peak concentrations of 218.9 and 223.0 µg L^{-1} were found at stations LFE02 and LFE04, respectively.

Before considering thin layers distributions and statistics, boundaries of the thin layers in each profile must be first defined. The upper and lower edges of the thin layers were identified as the depths at the full-width, half-maximum (FWHM) of the *chlorophyll a* profile peak (Cheriton et al., 2009). In other words, the upper and lower edges of the thin layers coincide with the upper and lower points that define the layer thickness, respectively (see Figure 4-8). The boundaries defined through the FWHM method allow capturing precisely the peak and the characteristics surrounding the peak. The defined boundaries of the thin layers were then used to distinguish along the characteristics related with the development of the thin layers observed above, between, and below the layers, i.e. buoyancy frequency, shear, turbulent dissipation rate, and all

other variables estimated over the vertical depth range of the thin layers. These data were then averaged for each profile.

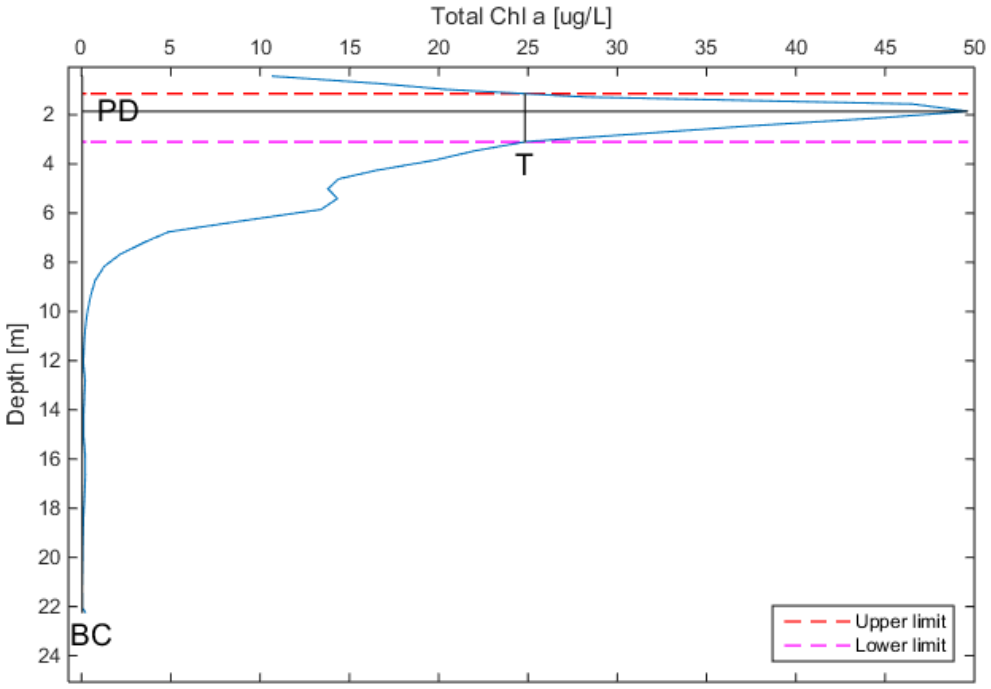

Figure 4-8 Example of parameters of a thin layer. Upper and lower depth boundaries of the thin layer are defined through the FWHM of the *chlorophyll a* profile peak (dashed lines). T represents layer thickness, BC background concentration, and PD peak depth.

Table 4-1 Parameters extracted from each identified thin layer.

Parameter	Stations				
	LFE02	**LFE03**	**LFE04**	**LFE05**	**LFE06**
Peak concentration (µg/L)	218.9	195.0	223.0	23.2	49.7
Peak depth (m)	1.3	1.3	3.2	2.7	1.9
Upper limit depth (m)	1.0	0.8	0.7	1.9	1.1
Lower limit depth (m)	2.2	2.2	3.8	3.9	3.1
Thickness (m)	1.2	1.3	3.1	2.0	2.0
Background concentration (µg/L)	71.1	13.1	65.0	2.4	0.1

4.3 Model calibration

In order to calibrate the hydrodynamic and ecological model ELCOM-CAEDYM, we defined the computational grid and the temporal step necessary to ensure precision and numeric stability of

the model. The model uses the Courant-Friedrichs-Lewy condition (CFL) to assess the stability of the numeric solution, values of CFL < 1 are required to consider stable the numeric solution.

Three simulations with the same configuration, time step, and vertical discretization were carried out in order to evaluate uniform horizontal grids of 25x25, 30x30, and 40x40 m. These grids were chosen based on previous studies with the model in other reservoirs. As a result, the CFL of the horizontal grid of 40x40 m cells presented instabilities in the solution with values of CFL > 1 (see Figure 4-9). For this reason the horizontal grid of 40x40 m cells was discarded and the analysis continue only with the horizontal grids of 25x25 and 30x30 m cells. Both grids presented a stable solution with values of CFL < 1 (see Figure 4-9). An analysis of the temporal evolution of temperature at each depth allowed to define the computational grid (see Figure 4-10).

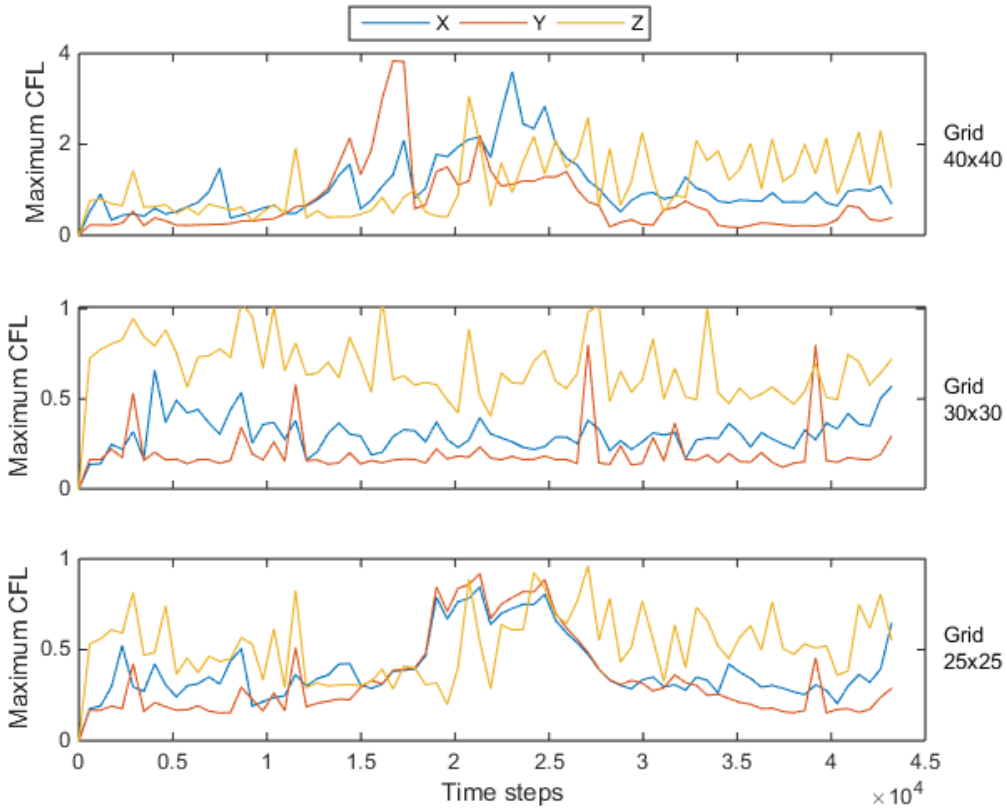

Figure 4-9 Maximum CFL in directions X, Y, and Z to three different horizontal grids.

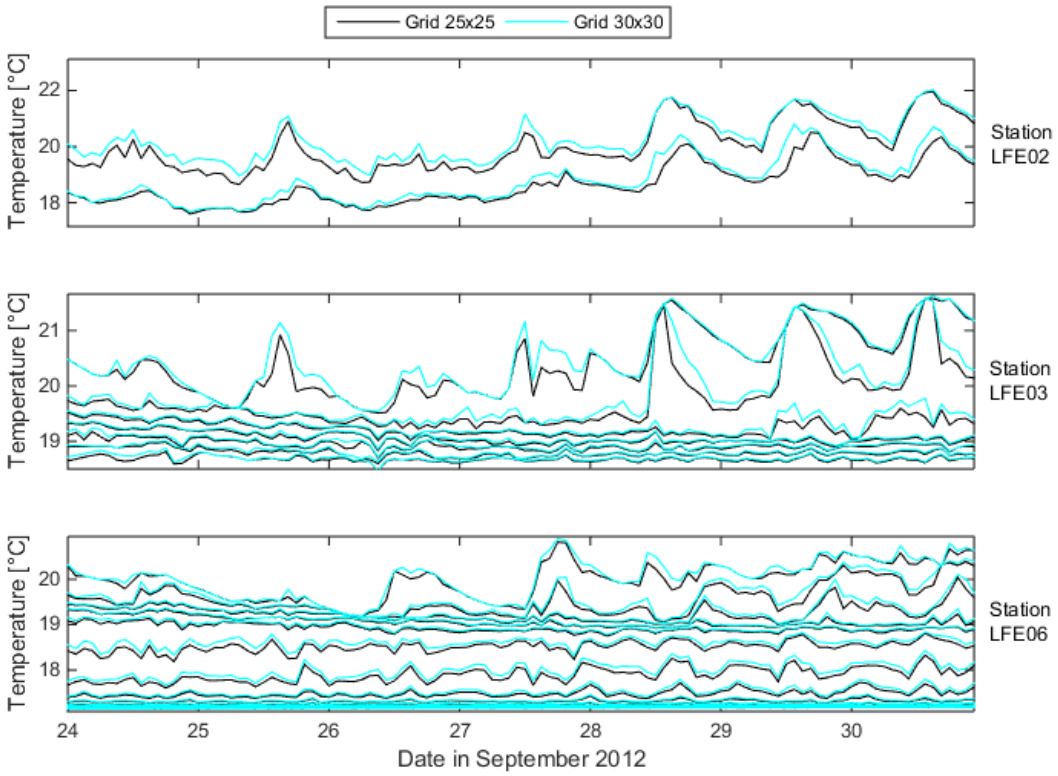

Figure 4-10 Temperature evolution simulated with horizontal grids of 25x25 and 30x30 m cells.

As observed in the figure, the simulated isotherms behaved similarly with both horizontal grids with more variability at surface as expected. These results showed that temperature differences due to the size of the horizontal grid were not significant. In this sense, each horizontal grid can be used to analyze the thermal structure of the reservoir. After evaluating uniform horizontal grids of 25x25, 30x30, and 40x40 m cells under the same model configuration, we have selected a uniform horizontal grid of 30x30 m cells based on the computational efficiency (shorter calculation time with regard to the horizontal grid of 25x25 m cells) and stability of the numeric solution.

An analysis of the vertical grid resolution of the model is required to adequately represent the fine–scale processes in the water column. We evaluated two vertical discretizations. In the first configuration, we used a discretization of 0.4 m thick layers in the shallower 12 m that then gradually increased up to 2.3 m thick layers in the deeper layers of the reservoir. This discretization divided the water column into a total number of 49 layers. In the second configuration, we used a finer vertical discretization of 0.2 m thick layers in the shallower 12 m and then a coarser discretization until 27.5 m depth. In this case, this discretization divided the water column into a total number of 79 layers. Both vertical discretizations were evaluated with the model. As a result, changes in the vertical grid resolution of the water column have no effect on temperature profiles as shown in the Figure 4-11. Therefore, the selection of the vertical grid

resolution to be used in the model will depend on the amount of information required at each cell to represent adequately the fine–scale processes in the water column.

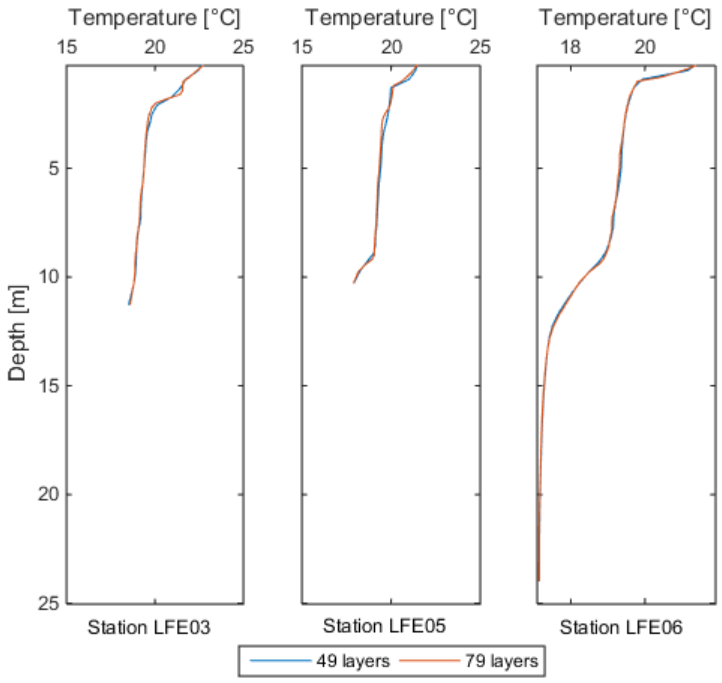

Figure 4-11 Temperature profiles with two different vertical grid resolutions.

Based on the scale at which the analyzed processes are developed, we selected a vertical grid resolution of 0.2 m thick layers in the upper part of the water column until 12 m depth and then a resolution with thickness gradual increments of 0.5, 0.7, 1.0, 1.2, 1.4, 1.7, and 2.3 m between 12 and 27.5 m depth. The maximum layer thickness was 2.3 m at the deeper layers of the reservoir. Thus, this vertical grid resolution divided the water column into a total number of 79 layers.

The time step at which the model resolves the hydrodynamic equations was also analyzed. As before, time steps of 30, 60, and 90 s were evaluated in terms of the CFL condition and the temporal evolution of temperature. In the three cases the CFL condition had values less than 1 during the entire simulation period in the three directions and the temperature profiles did not show significant differences between the evaluated time steps (data not shown). Based on these results, we chose a time step of 60 s as appropriate to carry out the simulations in terms of the balance between computational efficiency and stability of the numeric solution.

Once the numerical parameters were defined, the calibration of the model was performed adjusting the initial conditions and parameters related with temperature, dissolved oxygen, *chlorophyll a*, nutrients, and atmospheric conditions in the configuration files of the model. First, we will calibrate the hydrodynamic model adjusting the thermal structure and then based on the calibrated hydrodynamic model, we will calibrate the ecological module of the model.

Based on a previous calibration of the hydrodynamic model ELCOM, we simulated the temperature in the stations LFE02, LFE03, LFE04, LFE05, and LFE06 by adjusting the temperature profiles defined as initial conditions in each station and the parameters related with thermal structure in the reservoir. A uniform extinction coefficient of light and wind forcing were also included. The extinction coefficient of light was adjusted analyzing sensitivity of the results. On the other hand, the ecological model CAEDYM was calibrated adjusting biological parameters based on other similar studies which this model has been also applied (Carraro et al., 2012; Hillmer, Van Reenen, Imberger, & Zohary, 2008; Rigosi, 2010; Robson & Hamilton, 2004; Romero, Antenucci, & Imberger, 2004; Vidal et al., 2014) and analyzing the sensitivity of the results. Some of the modified parameters included: the maximum potential growth rate of phytoplankton, the light regimen, constant of saturation of nutrients, maximum and minimum concentration of nutrients, vertical migration parameters, nitrification and denitrification constants. The complete configuration file with the parameters and values used can be found in the Appendix. In addition, initial profiles of dissolved oxygen, *chlorophyll a*, and nutrients were included and distributed along the stations into the reservoir in order to reproduce the observed behavior of profiles in each station.

Thus, the hydrodynamics and water ecology of La Fe reservoir were simulated with the coupled model ELCOM-CAEDYM during a period of 30 days, starting on September 7th. Three different groups of phytoplankton were simulated with the model according to the groups identified in the reservoir: *cyanobacteria, cryptophytes,* and *freshwater diatoms*. Zooplankton species were not included in the model. The model was forced using temperatures and inflow rates of Las Palmas and Espíritu Santo, Boquerón and San Luis, and Pantanillo River at time scales of minutes, a few records of nutrients concentration in the inflows, and meteorological data from the meteorological station every 5 minutes. The initial temperature, dissolved oxygen, and *chlorophyll a* profiles were spatially distributed and defined from field data. Nutrients profiles were defined only to the station LFE06.

The calibration of temperature, dissolved oxygen, and *chlorophyll a* parameters is carried out in order to reproduce the observed profiles at specific times of the day in each station. Considering that the effect of the initial conditions imposed on the model disappears after 15 days of simulation, during the period of analysis the model reproduces well the temperature at the surface and the bottom of the water column as well as the spatial variability of the profiles (see Figure 4-12). Gradients are captured by the model mainly in the upper part of the water column. The simulated dissolved oxygen profiles adjusted well to the measured profiles as occurred with temperature (see Figure 4-12). Model results at the bottom of the water column were less accurate possibly due to the interactions that may exist with sediments as well as other processes occurred at the bottom that the model did not represent.

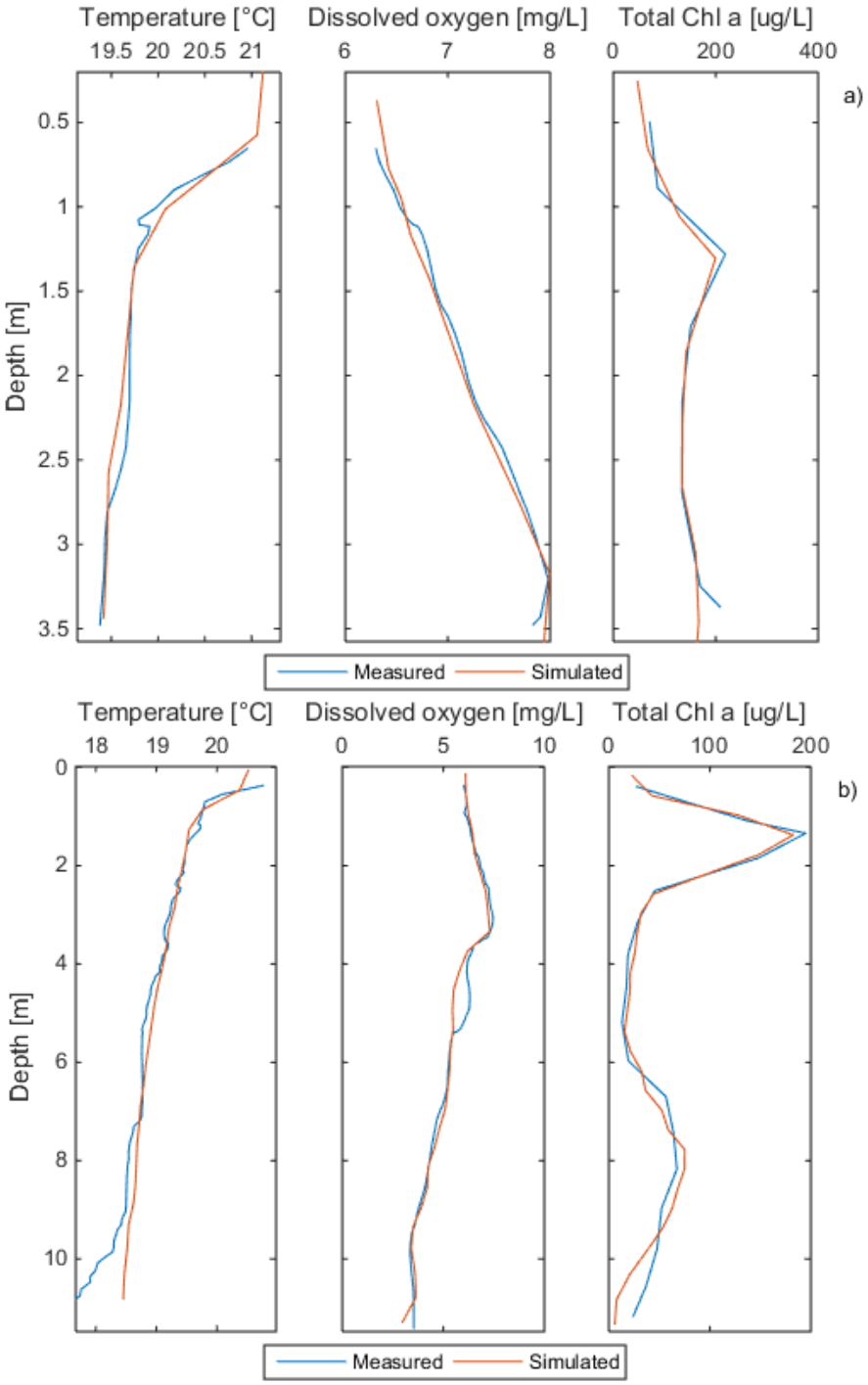
Temperature [°C]
Dissolved oxygen [mg/L]
Total Chl a [ug/L]
19.5 20 20.5 21
6 7 8
0 200 400
a)
Depth [m]
0.5 1 1.5 2 2.5 3 3.5
Measured
Simulated
Temperature [°C]
Dissolved oxygen [mg/L]
Total Chl a [ug/L]
18 19 20
0 5 10
0 100 200
b)
Depth [m]
0 2 4 6 8 10
Measured
Simulated

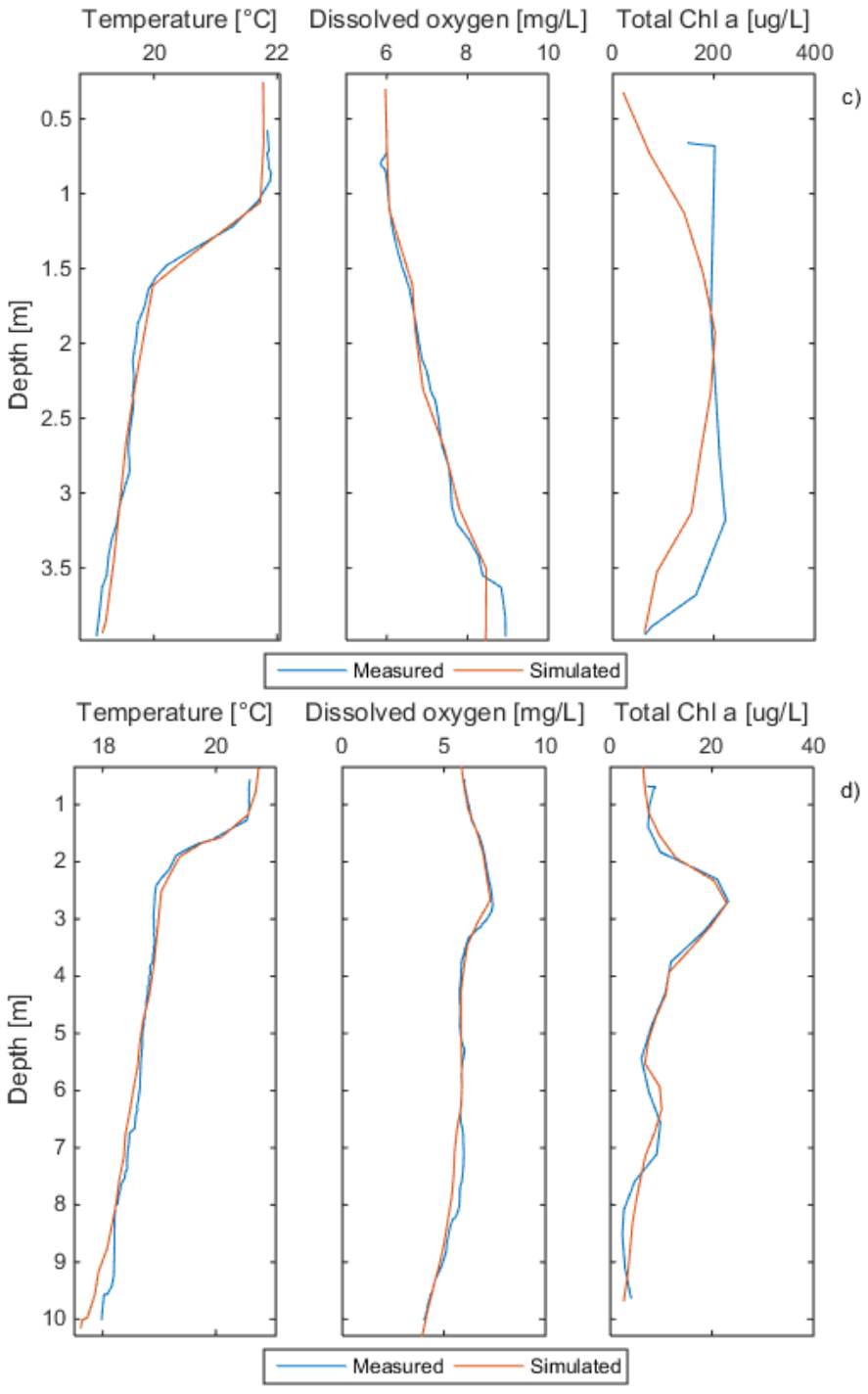
Temperature [°C]
Dissolved oxygen [mg/L]
Total Chl a [ug/L]
20
22
6
8
10
0
200
400
c)
0.5
1
1.5
2
2.5
3
3.5
Depth [m]
Measured
Simulated
Temperature [°C]
Dissolved oxygen [mg/L]
Total Chl a [ug/L]
18
20
0
5
10
0
20
40
d)
1
2
3
4
5
6
7
8
9
10
Depth [m]
Measured
Simulated

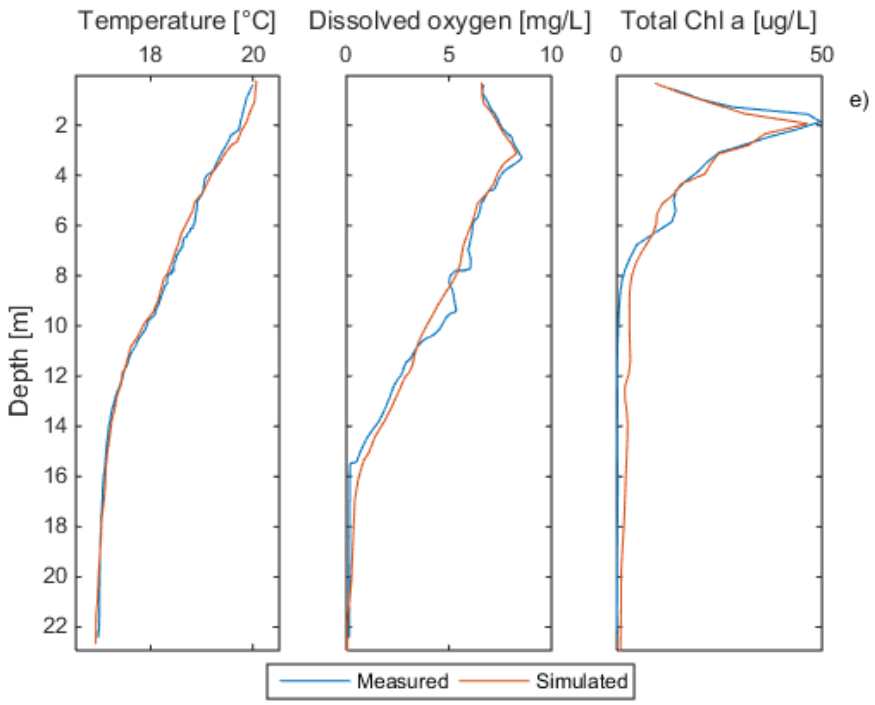

Figure 4-12 Temperature, dissolved oxygen, and total *chlorophyll a* profiles for stations a) LFE02 at 12:47 on September 25th, b) LFE03 at 10:44 on September 26th, c) LFE04 at 11:58 on September 26th, d) LFE05 at 13:59 on September 26th, and e) LFE06 at 10:16 on September 25th.

In the case of total *chlorophyll a* profiles, the model reproduces the depth of maximum peak concentration as well as the maximum concentration of each peak (see Figure 4-13). The main characteristics of each thin phytoplankton layer are also reproduced as shown in Table 4-2.

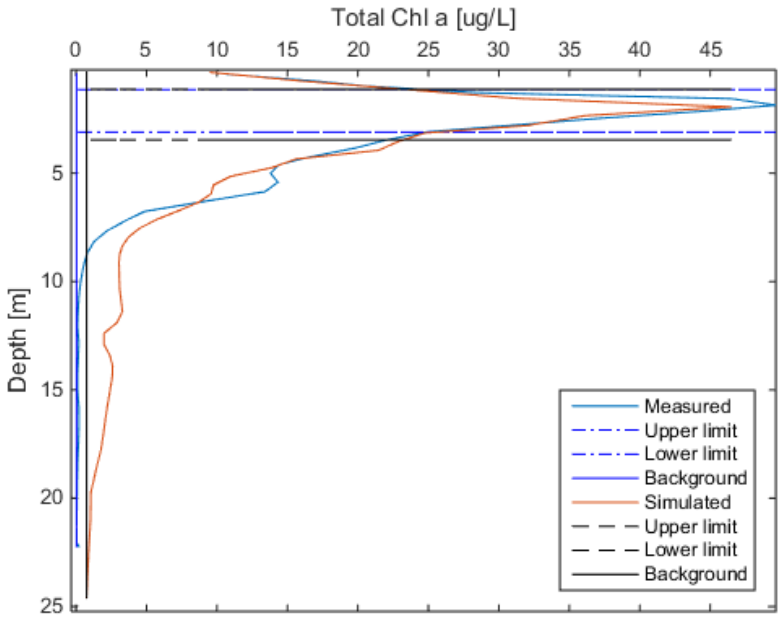

Figure 4-13 Thin layer parameters from the measured and simulated profiles of total *chlorophyll a* at station LFE06.

Table 4-2 Parameters extracted from each simulated thin layer.

Parameter	Stations				
	LFE02	**LFE03**	**LFE04**	**LFE05**	**LFE06**
Peak concentration (µg/L)	199,5	182,4	202,6	22,9	46,5
Peak depth (m)	1,3	1,4	1,9	2,7	1,9
Upper limit depth (m)	0,9	0,8	0,9	1,8	1,1
Lower limit depth (m)	2,3	2,2	3,4	4.0	3,5
Thickness (m)	1,4	1,4	2,6	2,2	2,3
Background concentration (µg/L)	47,3	5,9	21,5	2,6	0,8

Field data of velocities in the water column were not available. An approximation of these velocities can be carried out with the model, but first a validation of these approximations is required. For this, we analyzed the ability of the model to reproduce the behavior of the inflows using conductivity as a tracer (Vidal et al., 2011). Therefore, the comparison between conductivity and tracers profiles will give an idea of how well the model is representing the inflows, and associated to the inflows, the velocities into de water column. In this sense, we released three passive tracers with the same concentration into the main inflows of the reservoir: Tracer1 – Las Palmas and Espíritu Santo, Tracer2 – Boquerón and San Luis, and Tracer3 – Pantanillo River. The conductivity and simulated tracers profiles in each station are shown in the Figure 4-14.

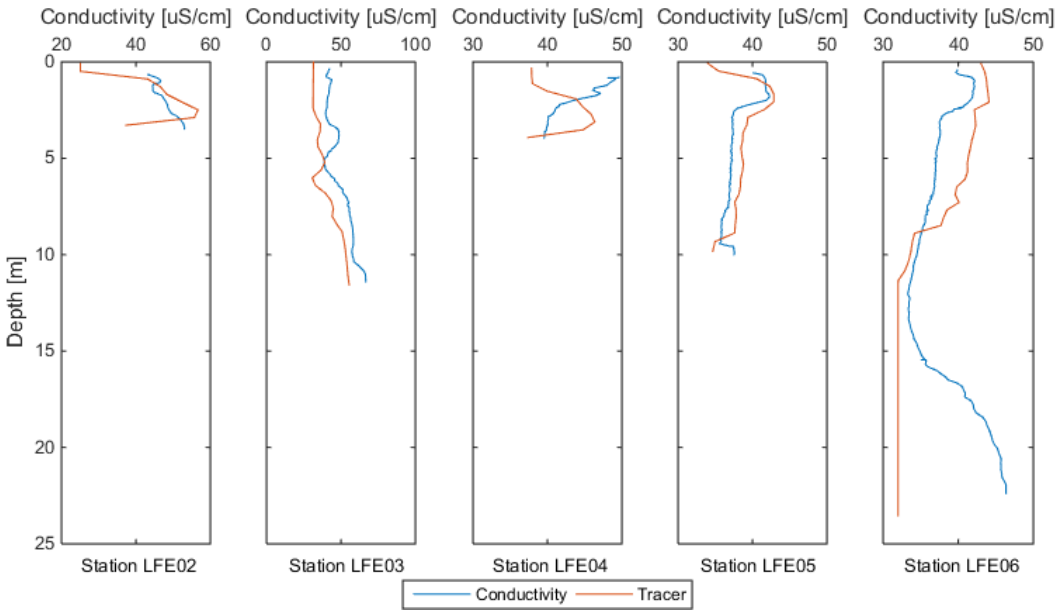

Figure 4-14 Conductivity and tracers profiles in each analyzed station.

As shown in the last figure, tracers were well represented by the model mainly in the upper part of the water column. The observed changes below the 14 m indicated water with different characteristics due to the accumulation of dissolved substances at these depths as reported by Román-Botero (2011). This accumulation of substances is not represented by the model, however the general characteristics of the conductivity profiles are well represented.

As a result of the rigorous calibration process of temperature, dissolved oxygen, and *chlorophyll a*, we achieved to reproduce the main characteristics of the water column at the specific hours of the day which the observed thin phytoplankton layers develop, and in this way, we obtained a coherent approximation to the velocities required to evaluate the mechanisms participating in the formations of the layers as described in the theoretical framework.

4.4 Layer maintenance and dissipation

Theoretical (e.g., Birch et al., 2008; Osborn, 1988) and in situ studies (e.g., Cowles et al., 1998; Cowles, 2003; Dekshenieks et al., 2001; Rines et al., 2002; Steinbuck et al., 2009), and numerical simulations (e.g., Franks, 1995) have demonstrated that vertical stratification and shear play an essential role in the formation and maintenance of vertical fine structures in the water column. We estimated the Richardson number as an indicator of the water column stability in order to determine the relationship between stratification and shear in the development of the observed thin layers in the reservoir. This number was calculated at each station in terms of the density estimated from the measurements and the velocities simulated with the model as presented in the theoretical framework.

As a result, we found that the squared vertical shear was relatively weak with values between 10^{-6} and 10^{-3} s^{-2}. Maximum values were found above and within the layers. Otherwise, squared buoyancy frequency was in the range of 10^{-5} and 10^{-2} s^{-2}. The Richardson number criterion was mostly higher than 0.25, this means that buoyancy becomes more important as the Richardson number increases (Stacey et al., 2007). Thereby, the stratification of the water column was stronger than the shear favoring the stability of the water column and the formation and maintenance of the observed thin layers. The squared vertical shear, squared buoyancy frequency, and Richardson number profiles are shown in the Figure 4-15. In this figure can be observed the similar behavior of N^2 estimated from measured profiles and simulated profiles with the model.

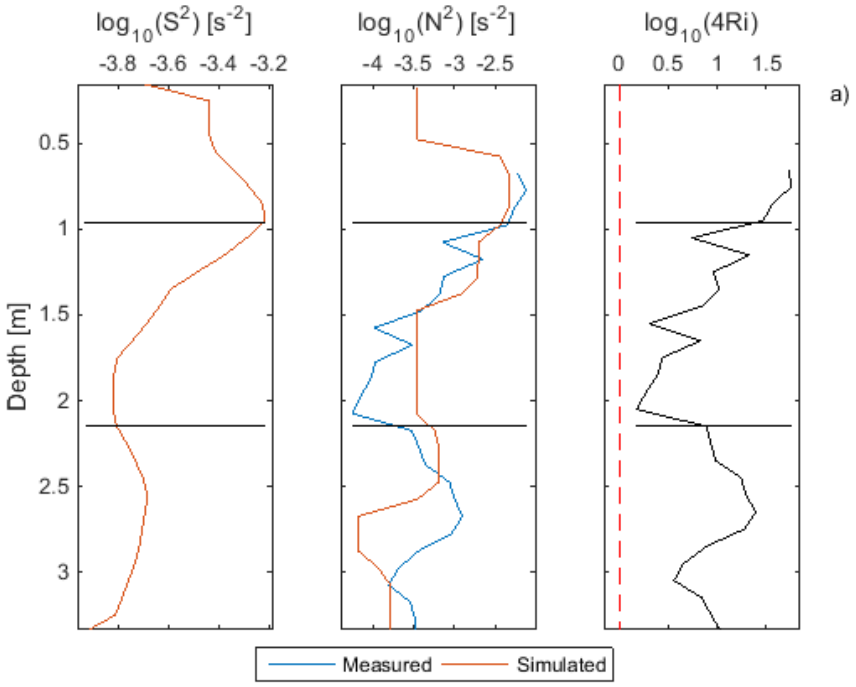
log10(S2) [s-2]
log10(N2) [s-2]
log10(4Ri)
-3.8 -3.6 -3.4 -3.2
-4 -3.5 -3 -2.5
0 0.5 1 1.5
a)
Depth [m]
0.5
1
1.5
2
2.5
3
Measured
Simulated

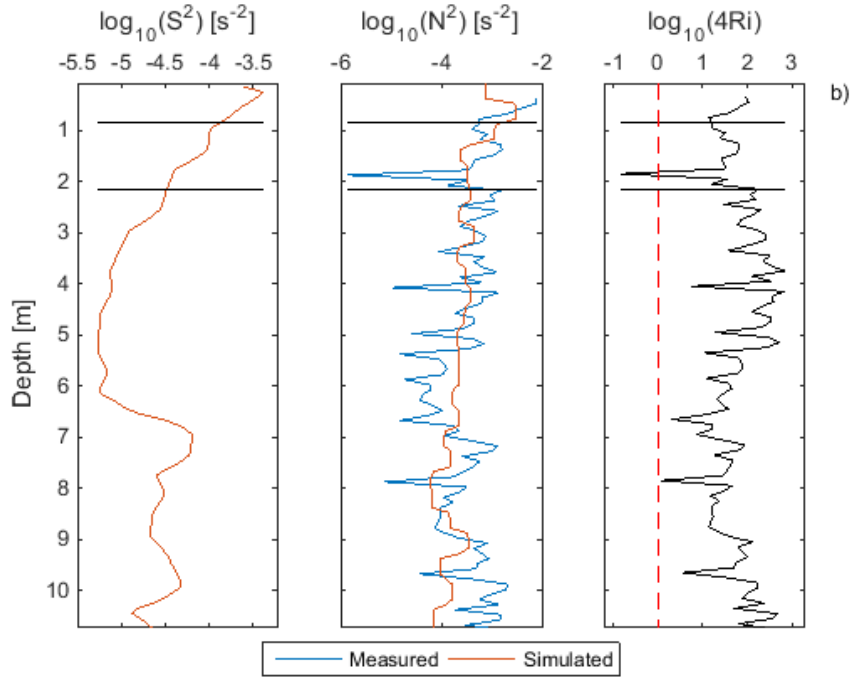
log10(S2) [s-2]
log10(N2) [s-2]
log10(4Ri)
-5.5 -5 -4.5 -4 -3.5
-6 -4 -2
-1 0 1 2 3
b)
Depth [m]
1
2
3
4
5
6
7
8
9
10
Measured
Simulated

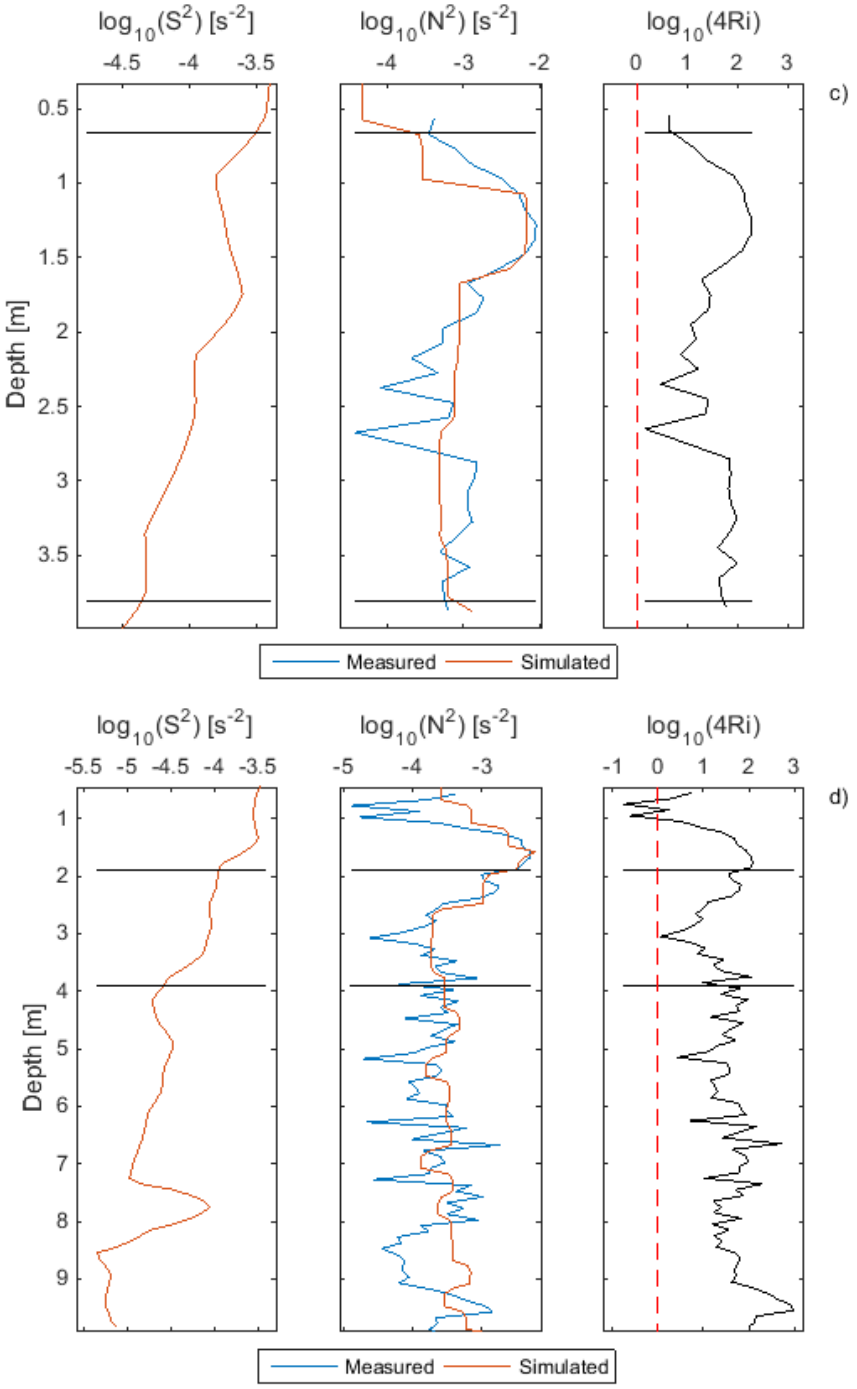
log10(S2) [s-2]
log10(N2) [s-2]
log10(4Ri)
c)
Depth [m]
Measured
Simulated
log10(S2) [s-2]
log10(N2) [s-2]
log10(4Ri)
d)
Depth [m]
Measured
Simulated

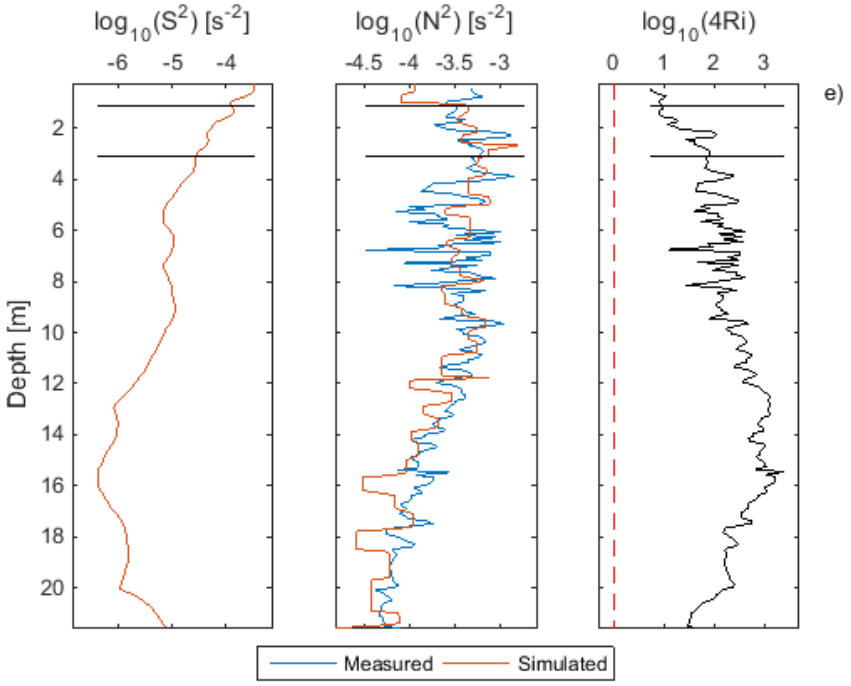

Figure 4-15 Squared vertical shear, squared buoyancy frequency, and normalized Richardson number profiles for each analyzed station: a) LFE02, b) LFE03, c) LFE04, d) LFE05, and e) LFE06. Thin layer edges are marked with a solid line in all panels. The red dashed line corresponds to a value of $Ri = 0.25$.

Because we do not have direct measurements of turbulence during the sampling period, the layer divergence was estimated through the turbulent dissipation rate calculated from the temperature profile at each station. Two methods were used. The first method determined the turbulent dissipation rate from the estimation of the Thorpe scale. An example of the Thorpe scale calculated from the temperature profile at station LFE03 is presented in the Figure 4-16. The second method calculated fluctuations of temperature from the temperature profile in each station. The mathematical procedure of both methods was described before in the theoretical framework. The values calculated by both methods are approximate and, in the case of the first method, based on the assumption that the Thorpe scale is approximately equal to the Ozmidov scale (Dillon, 1982; Gibson, 1980). This assumption has been confirmed by observations (Dillon, 1982) and it is according to the state of turbulence at maximal efficiency (Ivey & Imberger, 1991). Despite of the approximations made by both methods, results are in the same order of magnitude (see Figure 4-17).

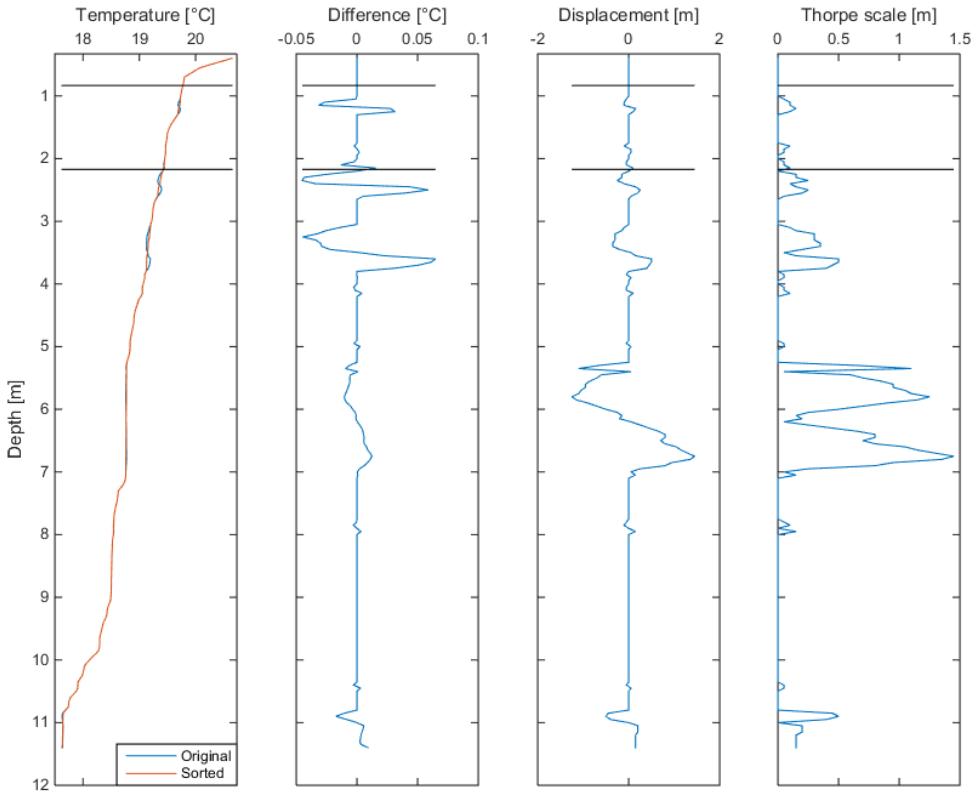

Figure 4-16 Example of the original and sorted temperature profiles, temperature difference between both profiles, displacement of water parcels, and the Thorpe scale for station LFE03. Thin layer edges are marked with a solid line in all panels.

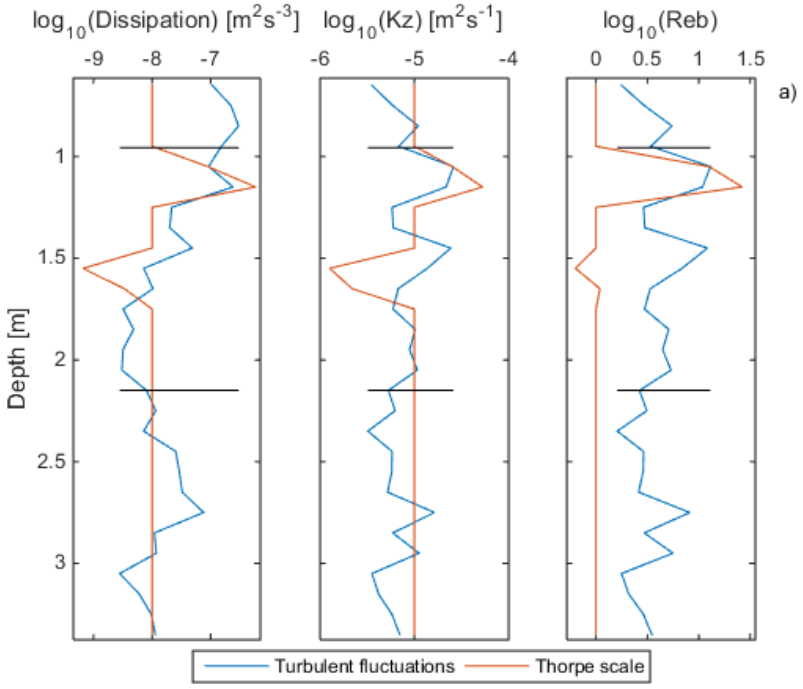

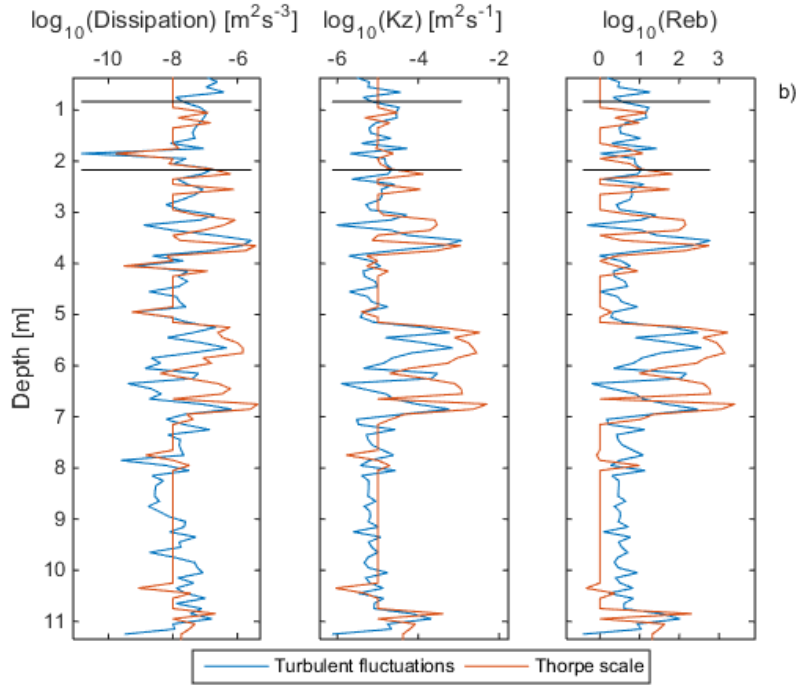
log10(Dissipation) [m2s-3]
log10(Kz) [m2s-1]
log10(Reb)
b)
Depth [m]
Turbulent fluctuations
Thorpe scale

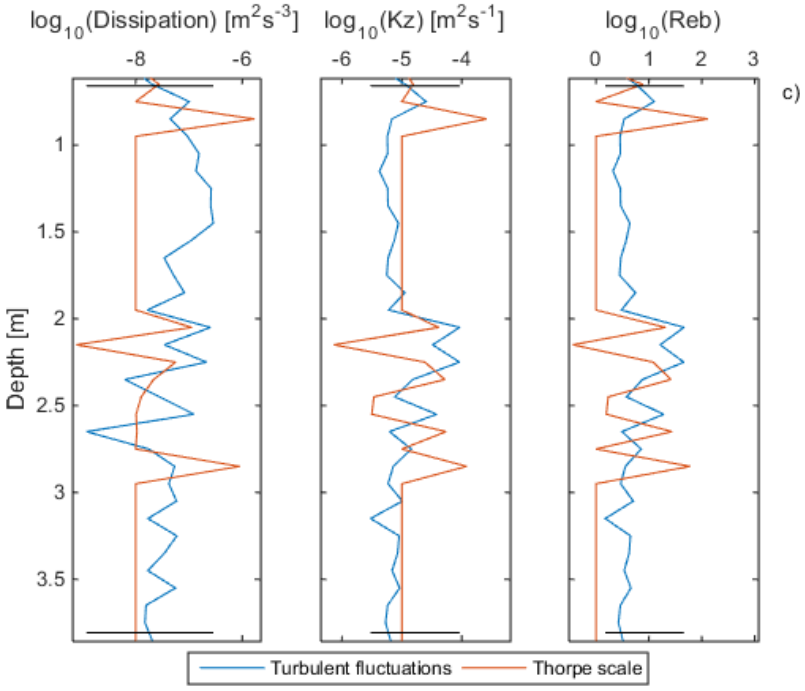
log10(Dissipation) [m2s-3]
log10(Kz) [m2s-1]
log10(Reb)
c)
Depth [m]
Turbulent fluctuations
Thorpe scale

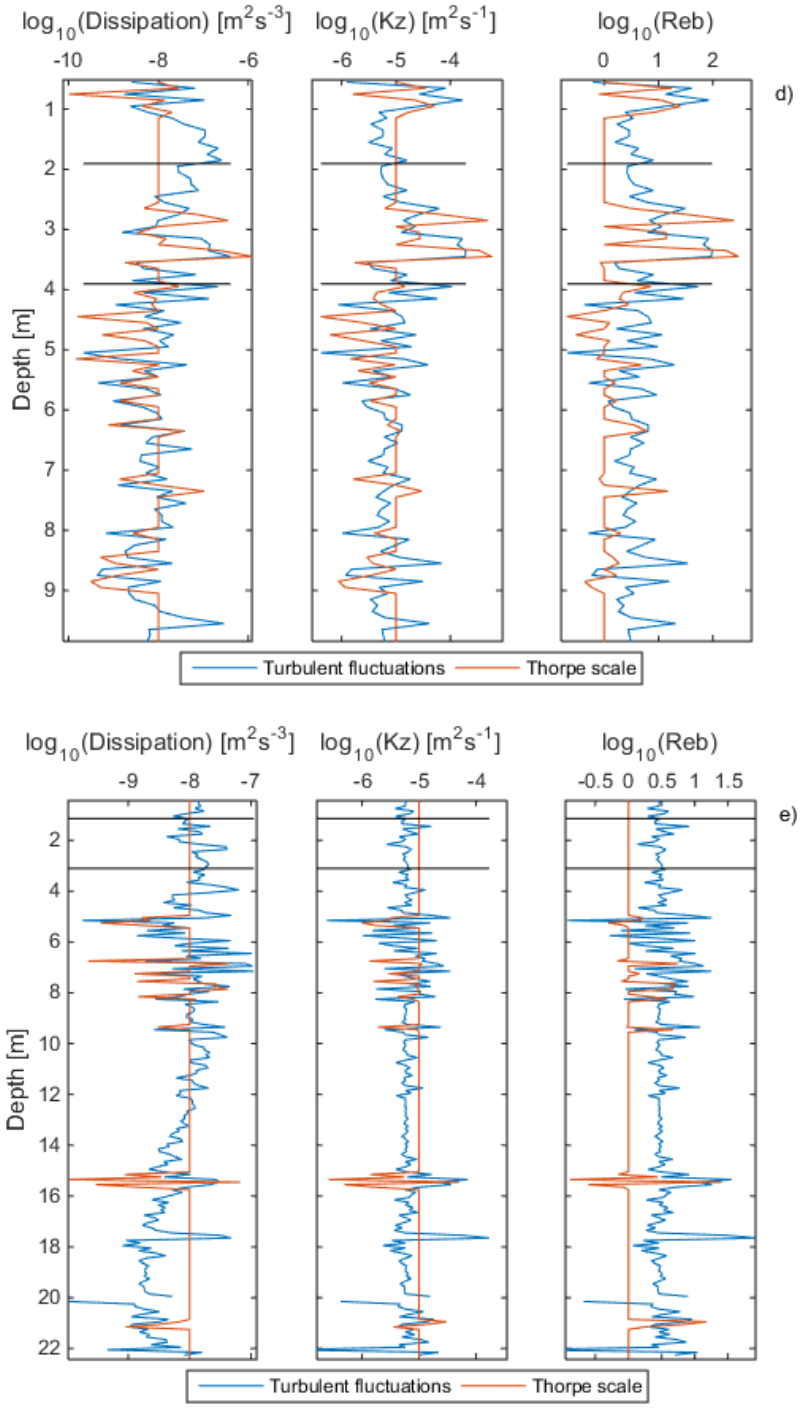

Figure 4-17 Dissipation, vertical turbulent diffusion coefficient, and buoyancy Reynolds number profiles estimated by Thorpe scale and turbulent fluctuations methods in each analyzed station: a) LFE02, b) LFE03, c) LFE04, d) LFE05, and e) LFE06. Thin layer edges are marked with a solid line in all panels.

Within the thin phytoplankton layers, turbulence intensity and mixing rates varied in different orders of magnitude. Dissipation rates were in general low within the layers with ε primarily in

the range of 10^{-9} and 10^{-7} m^2 s^{-3}. On the other hand, the vertical diffusion coefficients varied within the layer ranging from 10^{-6} to 10^{-3} m^2 s^{-1}. A large proportion of in-layer buoyancy Reynolds numbers were in the range of $Reb < \sim 15$, this means that stratification dominates turbulence at depths of the observed layers. The mixing conditions at the top and bottom of the layers in the water column were similar. The dissipation rates and the vertical diffusion coefficients were primarily between 10^{-9} to 10^{-6} m^2 s^{-3} and 10^{-6} to 10^{-3} m^2 s^{-1}, respectively. In general, buoyancy Reynolds numbers were in the range of $\sim 15 < Re_b < \sim 100$ indicating that turbulence was affected by stratification. In this sense, the obtained values of Reb represent the interaction between weak stratification and weak turbulence in the water column.

4.5 Layer convergence

We applied the scaling approach described in the theoretical framework in order to examine the mechanisms responsible for the formation of the observed thin layers. The evaluated mechanisms included convergent swimming, buoyancy, and in situ growth. First, we analyzed convergent swimming as the mechanism responsible for the formation of the observed thin layers. Based on the vertical diffusion coefficients estimated before and the thickness of each observed thin layer, we calculated the median swim velocities required for the phytoplankton species to maintain the layers under diffusion conditions. These velocities were in the range of 3.2 x 10^{-6} to 0.1 x 10^{-5} m s^{-1} (see Table 4-3). The estimated velocities were smaller than velocities typically reported in the literature for the phytoplankton species found in the reservoir (*Cyanobacteria, Cryptophytes,* and *Freshwater diatoms*) between 0.4 x 10^{-5} to 2 x 10^{-4} m s^{-1} (Reynolds, 1984; Vidal et al., 2014). According to these results, the observed layers should disperse in the water column due to the diffusion processes are stronger than the swimming velocities required for these species to form and maintain in the observed depths. Instead of this, the layers maintain in the water column. Therefore, the convergent swimming mechanism is not a clear candidate for the formation and maintenance of the layers at the observed depths.

Table 4-3 Parameters estimated for each evaluated mechanism. N: nitrogen, P: phosphorus.

Mechanism			**Stations**				
			LFE02	**LFE03**	**LFE04**	**LFE05**	**LFE06**
Convergent swimming ($w_{balance}$) [ms^{-1}]			9.8 e-06	9.9 e-06	4.7 e-06	0.1 e-05	3.2 e-06
Buoyancy ($D_{balance}$) [m]			4.4 e-04	5.1 e-04	1.9 e-04	5.8 e-04	2.3 e-04
In situ growth (ΔC_{obs} - ΔC_{growth}) [μgL^{-1}]	*Cyanobacteria*		51.7	27.3	55.3	4.17	17.4
	Cryptophytes		51.0	26.2	54.9	4.11	16.9
	Freshwater diatoms		52.5	28.2	55.8	4.26	17.5
In situ growth (T_{supply}) [days]	*Cyano.*	N	-	-	-	-	0.9
		P	-	-	-	-	20.2
	Crypt.	N	-	-	-	-	3.8
		P					90.7

	Fdiat.	N	-	-	-	-	0.9
		P					20.2

In order to examine buoyancy mechanism, we estimated the median diameters of phytoplankton cells required to balance the diffusive effect of turbulence on layer thickness. Accordingly with the theoretical framework, diameters were calculated in terms of the viscosity of water, vertical diffusion coefficient, buoyancy frequency, and thickness of each observed layer. The calculated diameters were in the range of 1.9×10^{-4} to 5.8×10^{-4} m (see Table 4-3). These values were higher than the diameters reported in the literature to *Cyanobacteria, Cryptophytes,* and *Freshwater diatoms* cells between 1×10^{-6} and 0.5×10^{-4} m. This difference between the diameters of the phytoplankton cells represents the unbalance between buoyancy-induced force and diffusive processes showing that the settling rate of phytoplankton cells is insufficient to counter turbulent mixing. Therefore, the buoyancy mechanism is unlikely to primarily contribute to the formation of the observed layers.

Now considering the potential formation of the layers by horizontal intrusions, we first analyzed the temperature and dissolved oxygen profiles in the different stations. Thin layers were colder and more oxygenated than the water immediately above in the water column, and warmer than the water below. Horizontal intrusions could explain the observed temperature and dissolved oxygen distributions as well as the *chlorophyll a* layers. The model was used to simulate the continuous release of passive tracers from the main inflows (Las Palmas and Espíritu Santo, Boquerón and San Luis, and Pantanillo River) into the reservoir. These simulations carried out during the period of analysis were developed to visualize at what depths and how the inflows (plumes) were transported along the analyzed stations (see Figure 4-18).

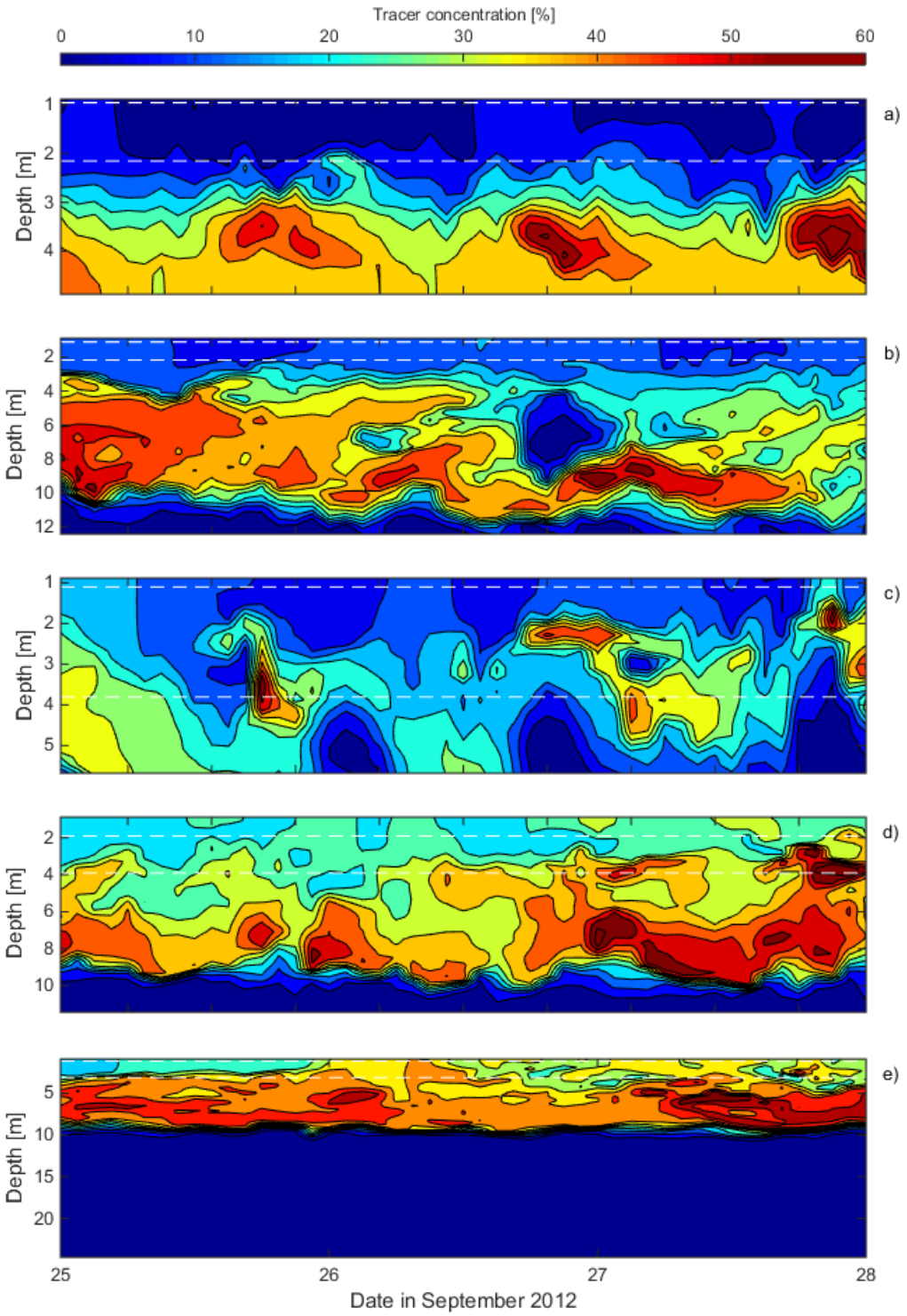

Figure 4-18 Temporal evolution of tracers concentration in each analyzed station: a) LFE02, b) LFE03, c) LFE04, d) LFE05, and e) LFE06. Thin layer edges are marked with a white dashed line in all panels.

In the upper meters of the water column, in a range similar to the described by Román-Botero (2011), were observed at stations LFE02 and LFE03 the plume of the inflow Las Palmas and Espíritu Santo and at station LFE04 the plume of the inflow Boquerón and San Luis. With respect to the plume of the Pantanillo River, we found that this plume moved in the upper 10 m of the water column according to the simulated results reported by Román-Botero (2011). However, in the same study Román-Botero (2011) demonstrated that the plume moved in the 14 meters depth which showed that the simulated plume of the Pantanillo River was not being completely represented by the model. The difference between measured and simulated results about the plume of the Pantanillo River may be due to the considerations made before related with the entrance of this inflow.

Comparing the depths of thin layers occurrence and intrusions we found that the broad range of depths at which intrusions develop did not coincide with the narrow range of depths of the observed thin layers. Therefore, the horizontal intrusion may not be considered as a mechanism contributing to thin layers formation by itself, but it may be considered as a trigger of other mechanisms such as in-layer growth. In order to analyze with more details the relationship between thin layers occurrence and intrusions, we considered the role of phytoplankton growth as a mechanism involved in the formation of the layers.

In-layer growth depends on the influx of nutrients through the water column. Here, we considered two potential supplies of nitrogen and phosphorus: horizontal intrusions and vertical turbulent fluxes. In the first scenario we examined whether intruding waters may carry nutrients that then stimulated phytoplankton growth according to Steinbuck et al. (2010). In this sense, we approximated the characteristic length scale of the patches through the simulated length observed of total *chlorophyll a* in each station (see Figure 4-19). Then, each characteristic length scale was used to estimate the horizontal dispersion coefficient for each layer. The resulting values ranged from 0.27 $m^2\ s^{-1}$ to 0.82 $m^2\ s^{-1}$.

Based on these estimations we calculated the increase in *chlorophyll a* concentration due to growth. The median values of ΔC_{growth} were less than ΔC_{obs} for all of the observed layers, however, the difference between them was acceptable considering the uncertainty associated to each parameter (see Table 4-3). The error percentages ranged between 15 and 37 percent. These results identify in situ growth as a possible mechanism involved in the layering process. This suggests that intrusions may contribute to the in-layer growth mechanism in the five analyzed stations through the supply of the nutrients required by phytoplankton to growth. The maximum net production rates of phytoplankton were 0.92, 0.80, and 1.06 day^{-1} for *Cyanobacteria, Cryptophytes,* and *Freshwater diatoms* respectively, according to Vidal et al. (2014) and the parameters reported in the model.

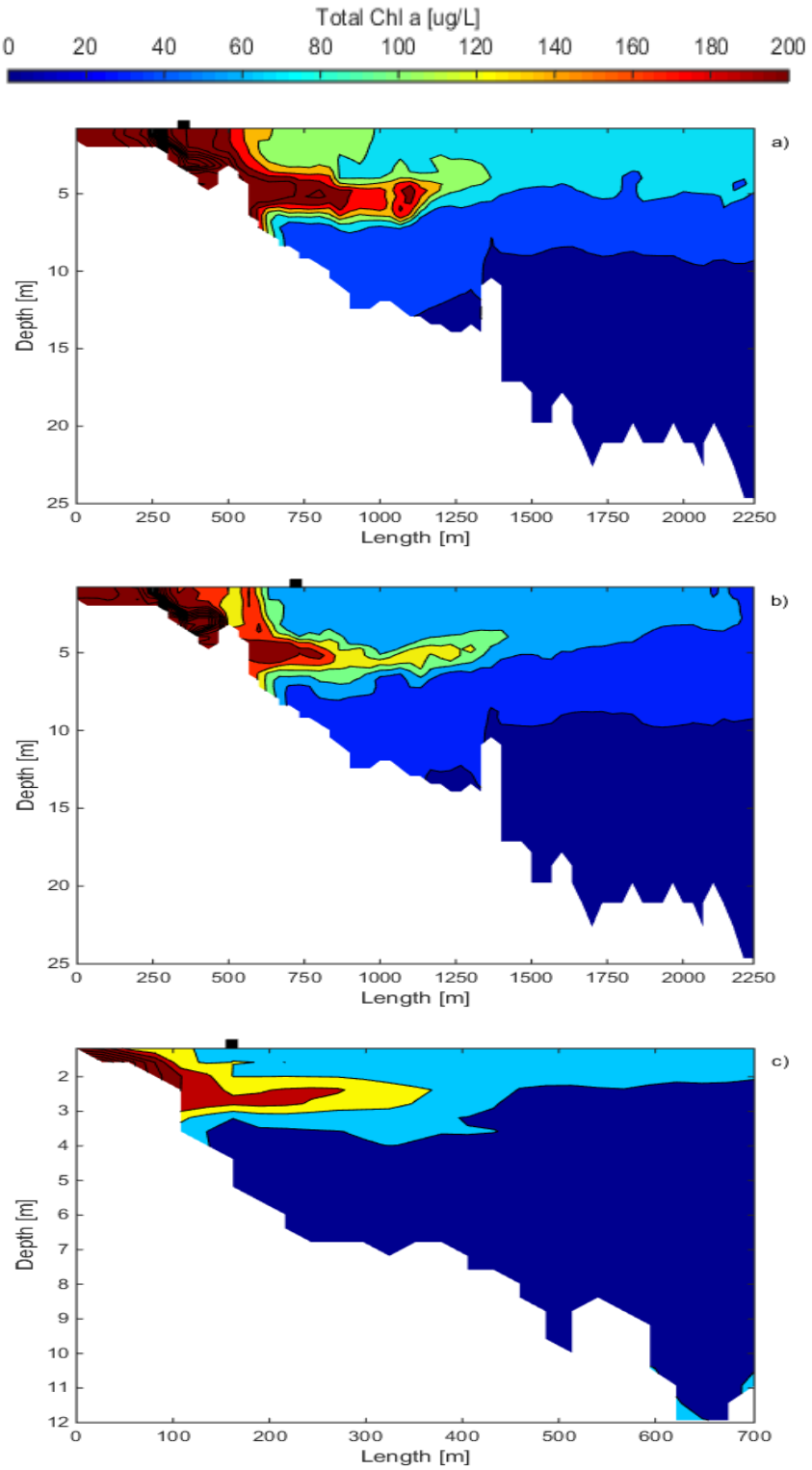
Total Chl a [ug/L]
0 20 40 60 80 100 120 140 160 180 200
a)
b)
c)
Depth [m]
Length [m]
0 250 500 750 1000 1250 1500 1750 2000 2250
0 100 200 300 400 500 600 700

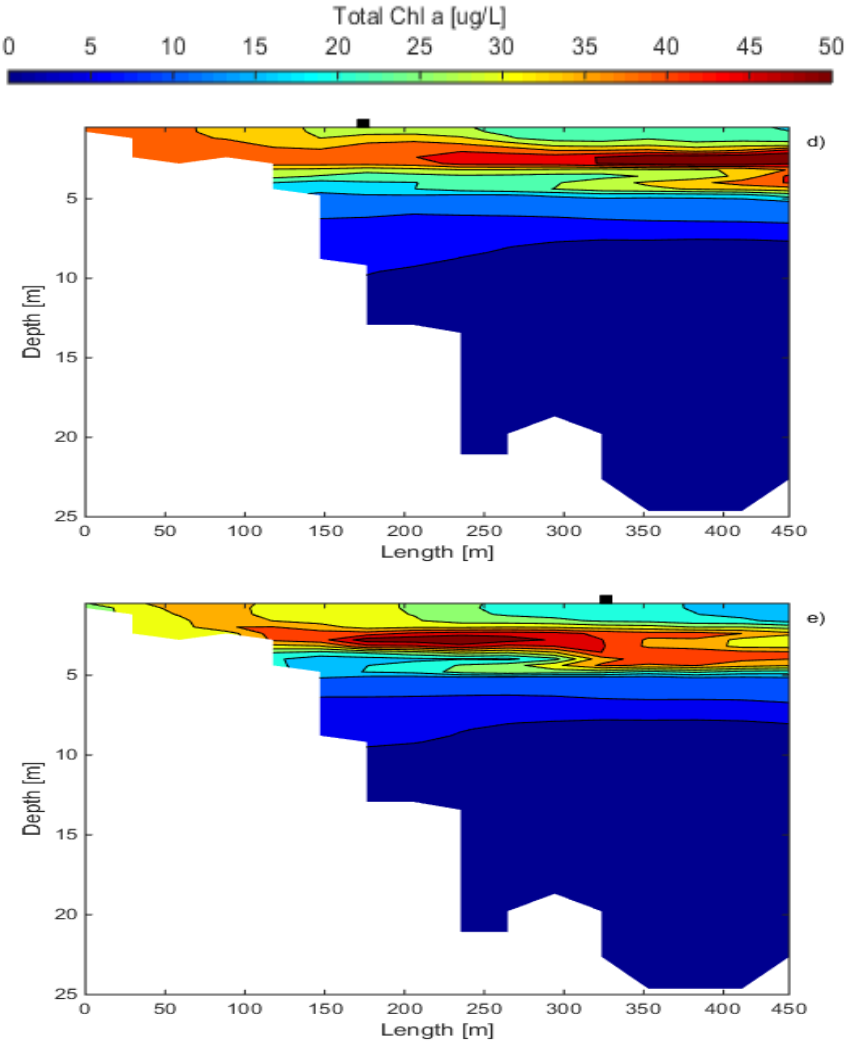

Figure 4-19 Characteristic length scale of the patches at stations: a) LFE02, b) LFE03, c) LFE04, d) LFE05, and e) LFE06. Contours were plotted from each station marked as ■ to the respective inflow at the observation time of the layers.

Now, we considered the supply of nitrogen and phosphorus from vertical turbulent fluxes as a factor stimulating growth. The vertical gradient of nitrogen and phosphorus was estimated from the measured nutrients at station LFE06. The upward vertical flux of nitrogen and phosphorus was at most 2.4 x 10^{-4} and 1.4 x 10^{-6} μgL^{-1} ms^{-1}, respectively. The values of the anomaly of the in-layer nitrogen and phosphorus nutrients (ΔN_{anom}) were calculated from the *chlorophyll a* anomaly of the layers according to Steinbuck et al. (2010). The *chlorophyll a* anomaly was estimated as the difference between vertically integrating *chlorophyll a* content of the observed layers and the background *chlorophyll a* content. Then, the amount of phytoplankton carbon was calculated from the ratio of carbon to *chlorophyll a* (C:Chl-a), whose values were 40, 180, 40 mg mg^{-1} for *Cyanobacteria, Cryptophytes,* and *Freshwater diatoms,* respectively, according to the configuration used in the model. Finally, the mass of phytoplankton carbon was converted to

moles of nitrogen and phosphorus using the molar mass of carbon and molar ratios for C:N:P according to the Redfield ratio, C:N:P=106:16:1 (Redfield, 1934).

The resulting timescales required for the supply of nitrogen were 0.9, 3.8, and 0.9 days for *Cyanobacteria, Cryptophytes,* and *Freshwater diatoms,* respectively (see Table 4-3). On the other hand, the timescales for the supply of phosphorus were 20.2, 90.7, and 20.2 days for *Cyanobacteria, Cryptophytes,* and *Freshwater diatoms,* respectively. Clearly, the timescales of phosphorus were too long compared to expected duration of thin layers in the water column. In the case of nitrogen, these results suggest that the vertical flux of nitrogen at station LFE06 was enough to stimulate the phytoplankton growth in the layer at the observed depth. Further, the proximity between the thin layer and the nitracline may favor such layered growth.

4.6 Thin layers development

In summary, thin phytoplankton layers were observed in stable regions of the water column, close to the mixed surface layer and above the stratified interior. The stratification at the top of the layers insulated the layers from the mixing above allowing the layers to persist. Thus, the strong influence of density in the water column created local regions with favorable conditions to the formation and maintenance of the observed phytoplankton layers as reported in other studies (Dekshenieks et al., 2001; McManus et al., 2003, 2005). In addition, the results showed that the low dissipation rates responsible to the turbulence around the layers were too low to disperse, erode or even broaden the layers contributing to layers maintenance.

Below the layers, stratification was also present and mixing rates were low. On the other hand, mixing was stronger in the upper meters of the water column where the flow may be affected by shear instabilities ($Ri < 0.25$). However, if these instabilities occurred, they were not strong enough to disperse the layers. The location of the layers coincided also with regions of strong temperature and dissolved oxygen gradients. All of these characteristics of the water column contributed to the formation of the layers. Owing to the layers occurred in the upper meters of the water column, the available of light was not considered as a limiting factor in the formation of the layers.

Based on the analysis of the mechanisms responsible of thin phytoplankton layers development, we have identified the possible mechanisms involved in the layering processes in the reservoir. We concluded that the formation of the layers was primarily triggered by the mechanism of in situ growth. This mechanism was favored by the fluxes and transport from the inflows (Las Palmas and Espíritu Santo, Boquerón and San Luis, and Pantanillo River) of the nutrients required by the phytoplankton cells to growth forming the observed layers. In the five analyzed stations the growth of phytoplankton cells due to the supply of nutrients from intruding waters may be considered as a possible mechanism of layer formation. The growth of phytoplankton cells due to the fluxes of nutrients in the water column could also be verified at the deeper station (LFE06). In this station the increased amount of nutrients in the layer, specifically nitrogen due to the vertical

fluxes generated in the water column, will stimulate phytoplankton growth and contribute to the formation of the thin layer as observed in the measured profile of *chlorophyll a*. The rainfall event occurred at the afternoon of 24th of September could contribute to the availability of nutrients in the water column increasing fluxes and transport from the inflows, thereby stimulating the growth of phytoplankton cells at the observed depths.

Mechanisms such as convergent swimming and buoyancy were discarded as the primarily mechanisms responsible of the formation of the layers, however, it does not mean that these mechanisms not participated in another period of time or location in the formation of layers due to these mechanisms depend particularly on the water conditions and specific phytoplankton species in the water column. Thereby, the formation of the layers at the specific observed depths and locations in this study was a consequence of the interaction between the analyzed mechanisms, the stratification and turbulence conditions around the formed layers, and the specific requirements of the phytoplankton cells at the different stations.

Here, we have developed our analysis in terms of the more common mechanisms observed in layer formation, i.e. convergent swimming, buoyancy, and in situ growth. An analysis of other mechanisms such as straining involves the definition of parameters as the initial conditions of the patch, the interactions of the strained patch with the organisms around it, and the complete length of the strained patch. All these parameters must be taken into account to the detailed analysis of this mechanism. In our case, the knowledge about these parameters limited our analysis due to the impossibility with the data available or the model to calculate them and then demonstrate the participation of this mechanism in the formation of the observed layers.

The development of thin phytoplankton layers was probably influenced by more than one mechanism, however, we have assumed that each of these mechanisms acts independently and is essentially homogeneous, in addition to the other assumptions made in each mechanism. The validity of these assumptions will depend on the scale at which the physical parameters vary. Even if the parameters present some vertical variation, a first approximation like this is likely to be appropriate to define layers characteristics. In this sense, the simplifying assumptions together with our limited field data restricted our analysis to the more basic case of thin layers formation, maintenance and dissipation, considering our analysis as an approximation to the study of the mechanisms acting in the reservoir.

In spite of the particular characteristics of thin layers observed in this study, our results were in agreement with those of similar thin layers studies. We associated the development of thin phytoplankton layers to the stratified conditions of the water column together with the destabilize effect of shear instabilities according to Dekshenieks et al. (2001) and McManus et al. (2003,2005). They found that observed thin layers occurred in regions where the Richardson number was >0.25, which is consistent also with other studies (Cheriton et al., 2007; Prairie et al., 2010; Sevadjian et al., 2010; Steinbuck et al., 2009).

In our analysis we followed the study conducted by Steinbuck et al. (2010) which they defined that the observed layers may have formed from horizontal intrusion of water with elevated phytoplankton concentrations. We coincided with this study and previous ones in the fact that layers occurred in density stratified regions with variables rates of turbulent mixing as well as in the necessity of detailed measurements to evaluate the potential processes involved in thin layers development.

With regard to other studies related with the development of thin layers, Franks (1992) developed a model to explain the enhanced biomass through the interactions of floating, sinking or swimming with the flow whilst Stacey et al. (2007) provided a framework extending Franks' (1995) analysis of kinematic straining to include turbulent mixing into the analysis of straining, motility and buoyancy mechanisms. Birch et al. (2008) described plankton distributions in terms of four phases of layer evolution and plankton growth, and then Birch, Young, & Franks (2009) following the previous work of Stacey et al. (2007) analyzed in detailed the form of the peaks produced by straining, motility and buoyancy mechanisms. Recent studies about the mechanisms responsible of the formation of thin layers were reported by Steinbuck et al. (2009,2010) in which they evaluated in the earlier study an Eulerian advection–diffusion model and Lagrangian particle-tracking model to explain the formation of thin layers, and then in the second study they analyzed the fine-scale phytoplankton layer dynamics in the context of turbulent mixing. Despite to the diverse studies about the mechanisms involved in the development of thin layers, in each case the approach to identify the mechanisms participating in the formation of the layers was different due to the specific conditions, assumptions, data, models and unique characteristics of each observed thin layer. All of those approaches showed the broad uncertainty associated with the definition of the mechanisms governing layer dynamics and the gaps in theory that we still have and need to complement in order to understand, identify and define with more details thin layers mechanisms and characteristics.

With this in mind, our study sought to provide elements to understand how the observed thin layers developed in La Fe reservoir. Understanding of layer dynamics and the factors governing it may help to develop mathematical models and scaling parameters capable to represent and estimate more appropriately phytoplankton distributions and blooms as well as predict the impacts of these layers in the ecosystems. Besides, if we know how and where thin phytoplankton layers develop we could control the factors influencing a specific event and in this way disrupt its propagation. Taking into account that the water in La Fe reservoir is primarily to the supply of drinking water, this kind of studies are essential to preserve the quality of water in the reservoir.

Particularly, in Colombia a study of these characteristics had not done before. In this sense, this study may contribute to the generation of new projects in order to broad the knowledge about thin phytoplankton layers dynamics in Colombia and in general, in tropical scenarios. Taking into account that there are only a few studies related with the governing mechanisms of thin layers development in reservoirs, and even less in tropical reservoirs, the results of this study may also

contribute to the discussion of the scientific community about phytoplankton dynamics in terms of the difference between tropical, middle and high latitude systems.

5. Conclusions

In this study, thin phytoplankton layers development was considered in the context of turbulent mixing. Layers were observed within the upper water column at depths between 0 and 5 m, in density-stratified regions with different rates of turbulent mixing. In general, these layers were limited by a turbulent surface layer and a weakly turbulent, stratified interior. Thin layers were mainly associated to the stable conditions of the water column. Besides, these layers persisted in the water column because the turbulence acting to broaden the layers was insufficient to disrupt the layers for prolonged periods of time. As other studies, we recognized the necessity of detailed measurements of turbulence and specific parameters to adequately define the mechanisms participating in the development of the layers. The methods used to estimate the turbulent dissipation rates gave similar results, however, these values must be considered as an approximation of the real ones due to the natural variability of dissipation rates and the inherent uncertainty associated to the assumptions made.

With regard to the simulation results, the model ELCOM-CAEDYM reproduced well at the observation time of the events the hydrodynamic conditions and phytoplankton layers in the five analyzed stations in the reservoir. Despite to the lack of velocity data, the results obtained from the model were coherent with the field observations and previous studies. In this sense, the results were an acceptable approximation to the real ones. These results showed the good performance of this model simulating a stratified reservoir as well as its potential as a tool to analyze layers distributions after an adequately calibration, and if possible, validation. Despite of the results of the model, the calibrated parameters only apply to the specific events analyzed. More field data at different spatial and temporal scales are required to calibrate and validate this model, and in this sense, use it to predict the behavior of the reservoir under different environmental conditions and events.

The scaling analysis showed that convergent swimming and cell buoyancy were not the primarily candidate mechanisms for layer formation and maintenance, but eventually, these mechanisms could participate under other conditions in the water column. Instead, the results indicated that the layers may have formed primarily from in situ growth mechanism. Based on the scaling analysis, we showed that intrusions may contribute to the formation of the layers influencing in-layer growth mechanism. In this sense, in-layer growth stimulated by nutrient-rich intrusions and vertical turbulent fluxes of nutrients was responsible to produce the observed phytoplankton

layers. This conclusion showed the fundamental role of inflows in the definition of the water dynamics in a reservoir, and specifically, in the formation of phytoplankton layers.

Although we cannot determine the exact mechanisms by which the observed thin phytoplankton layers were formed in the reservoir, we were able to identified possible mechanisms by analyzing the concurrent physical, chemical, and biological data. Further studies are required to define more appropriately the mechanisms involved in the formation of layers as well as its characteristics (initial patches dimensions, tilt angles, swimming velocities, species diameters, nutrient fluxes). The melding of theory, field observations and numeric simulations pursued in this study showed how these different ways to face the identification of mechanisms can be coupled in order to achieve a deeper understanding of thin layers development.

6. Recommendations and future work

This study provided a mechanistic approximation to the mechanisms governing phytoplankton layers formation, maintenance, and dissipation in La Fe reservoir. It would be highly desirable to complement this approach with direct and detailed observations of velocities and turbulent dissipation rates as well as measures at diurnal and monthly scales that allow a more complete description and evaluation of the layering mechanisms (e.g., initial patches dimensions, tilt angles, swimming velocities, species diameters, nutrient fluxes). These measures will contribute to build more definitive conclusions about the mechanisms involved in layering processes. Considering even other processes occurred in the water column will complement our analysis and contribute to better insights about the thin layer characteristics, dynamics, and associated environmental conditions.

The mechanisms reviewed in this study not include the effects generated by the contraction and expansion of isopycnals and other divergent mechanisms that contribute to the dissipation of the layers. These effects could be incorporated, in the first case, with the addition of an additional term on the balance equations to account for the waves responsible of the changes on isopycnals. Other divergent mechanisms, different to the homogeneous turbulent diffusion considered here, include diffusive (undirected) swimming and out migration from the layer (directed swimming) (Stacey et al., 2007). In each case, a velocity scale could be defined in order to quantify the rate of layer thinning or thickening. This velocity could be then incorporated in the analyzed scaling framework.

Besides, other mechanisms such as straining, gyrostatic trapping, and differential grazing can be studied in order to include more mechanisms into the analysis. An analysis of other velocity scales for vertical swimming velocity of phytoplankton species as proposed by Birch et al. (2009) and for the settling velocity used in the buoyancy mechanism may contribute to the understanding of layers development and the discussion about this scaling framework. On the other hand, the considerations and simplifying assumptions made in each mechanism have to be revised in detail in order to study more real phytoplankton events and interactions into the water column.

It would be interesting to apply the scaling approach of these mechanisms in other tropical reservoirs and environments in order to test the universality of the proposed analysis. Thereby, further studies are needed to understand the dynamic of the layers and the factors that influence it as well as to develop methods to quantify the relative participation of each mechanism in the formation of the layers.

Appendix: CAEDYM parameters

PHYTOPLANKTON constants			
	CYANO	**CRYPT**	**FDIAT**
Maximum potential growth rate of phytoplankton (Pmax) [/day]	0.64	1.48	1.80
Average ratio of C to chlorophyll a (Ycc) [mg C/mg chla]	40	180	40
Light limitation			
Type of light limitation algorithm (2=no photoinhibition, 3=photoinhibition) (algt) [no units]	2	3	3
Parameter for initial slope of P_I curve (IK) [microE/m^2/s]	140	40	60
Light saturation for maximum production (ISt) [uE$m^{-2}s^{-1}$]	1300	200	120
Specific attenuation coefficient (Kep) [ug chla$L^{-1}m^{-1}$]	0.1264	0.0890	0.0140
Nutrient parameters			
Half saturation constant for phosphorus (KP) [mg/L]	3.00E-4	3.00E-2	3.00E-2
Low concentrations of PO_4 at which uptake ceases (Po) [mg/L]	0.0	0.0	0.0
Half saturation constant for nitrogen (KN) [mg/L]	8.46E-2	2.00E-2	4.00E-2
Low concentrations of N at which uptake ceases (No) [mg/L]	0.0	0.0	0.0
Constant internal Silica concentration (Sicon) [mg Si/mg Chla]	0.0	0.0	120
Half saturation constant for silica (KSi) [mg/L]	0.0	0.0	0.44
Low concentrations of Si at which uptake ceases (Sio) [mg/L]	0.0	0.0	0.01
Half saturation constant for carbon (KCa) [mg/L]	2	2	2
Minimum internal N concentration (INmin) [mg N/mg Chla]	2.5	3.0	5.6
Maximum internal N concentration (INmax) [mg N/mg Chla]	5.0	9.0	7.5
Maximum rate of phytoplankton nitrogen uptake (UNmax) [mg N/mg Chla/day]	1.5	1.5	15.0

Minimum internal P concentration (IPmin) [mg P/mg Chla]	0.40	0.30	0.25
Maximum internal P concentration (IPmax) [mg P/mg Chla]	0.8	1.5	1.0
Maximum rate of phosphorus uptake (UPmax) [mg P/mg Chla/day]	0.20	0.04	0.14
Minimum internal C concentration (ICmin) [mg C/mg Chla]	15	15	15
Maximum internal C concentration (ICmax) [mg C/mg Chla]	80	80	80
Maximum rate of carbon uptake (UCmax) [mg C/mg Chla/day]	50	50	50
Constant Internal P ratio if no int P is modelled (IPcon) [mg P/mg Chla]	0.1	0.3	0.1
Constant Internal N ratio if no int N is modelled (INcon) [mg N/mg Chla]	2	3	2
Maximum nitrogen fixation rate (NFixationRate) [mg N/mg Chla /day]	2	2	2
Growth rate reduction under maximal N fixation (gthRedNFix)	1	1	1
Temperature representation			
Temperature multiplier (vT) [no units]	1.092	1.080	1.060
Standard temperature (Tsta) [Deg C]	20.0	-6.4	16.0
Optimum temperature (Topt) [Deg C]	28	-29	20
Maximum temperature (Tmax) [Deg C]	35.00	-0.05	29.00
Respiration mortality and excretion			
Respiration rate coefficient (kr) [/day] & (krp) []	0.08 0.00	0.20 0.00	0.10 0.00
Temperature multiplier (vR) [no units]	1.068	1.095	1.070
Fraction of respiration relative to total metabolic loss rate	0.7	0.7	0.7
Fraction of metabolic loss rate that goes to DOM (rest goes to POM)	0.7	1.0	0.7
Salinity limitation			
Maximum potential salinity (maxSP) [psu]	36	36	36
Type of water environment (phsal) [no units]	0	0	0
Minimum bound of salinity tolerance (Sop) [psu]	3	1	1
Salinity limitation value at S=0 and S=maxSP (Bep) [no units]	3	2	5
Salinity limitation value at S=Sop (Aep) [no units]	1	1	1
Vertical migration and settling			
Type of vertical migration algorithm (0-stokes, 1-constant, 2-motile 3-motile with photoinhibition) (phvel) [no units]	2	3	1
Rate coefficient for density increase (c1) [kgm^{-}	0.2	0.9	0.9

$^{3}min^{-1}$]			
Minimum rate of density decrease with time (c3) [$kgm^{-3}min^{-1}$]	0.0500	0.0415	0.0415
Rate for light dependent migration velocity (c4) [mhr^{-1}]	0.30	0.85	0.85
Rate for nutrient dependent migration velocity (c5) [mhr^{-1}]	0.30	0.65	0.65
Half saturation constant for density increase (IKm) [$uEm^{-2}s^{-1}$]	278	25	25
Minimum phytoplankton density (min_pd) [kg/m^3]	990	980	980
Maximum phytoplankton density (max_pd) [kg/m^3]	1002	1050	1025
Density of water at 20 deg C (pw20) [kgm^{-3}]	1000		
Diameter of phytoplankton (dia) [m]	0.15E-03	0.10E-04	0.10E-04
Constant settling velocity (ws) [ms^{-1}]	1.12E-06	-0.36E-05	-6.72E-05
DO threshold which motile phytos will not migrate below (oth) [mg O/L]	0.0	0.0	0.0
Resuspension			
Critical shear stress (tcpy) [N/m^2]	0.001	0.001	0.001
Resuspension rate constant (alpPy) [mg $Chla/m^2/s$]	0.008		
Controls rate of resuspension (KTPy) [mg $Chla/m^2$]	0.01	0.01	1.00
Phytoplankton sediment survival time (DTphy) [days]	2	2	2
Algal toxin and metabolite dynamics			
Internal metabolite conc when growth is zero (IXmin) [mg/L (mg Chla/L)$^{-1}$]	0.2	0.0	0.0
Internal metabolite conc when growth is Pmax (IXmax) [mg/L (mg Chla/L)$^{-1}$]	2.0	0.0	0.0
Temperature decay constant for metabolites (mX)	0.01	0.0	0.0

OXYGEN constants	
Maximum limit of polychaete biomass (PCmax) [g/m^2]	50
Respiration stoichiometric ratio of C to O_2 (YOC) [mg C/mg O]	2.66667
Frac of net DO allocated to seagrass roots (fox) [no units]	0.10
Stoichiometric factor, seagrass C : DO (YSG) [mg sgC/mg O]	2.66667
Stoichiometric factor, jellyfish C : DO (YOJ) [mg jelC/mg O]	2.66667

Minimum DO in the bottom layer (mg/L) (oxmin) [mg/L]	0.03
Photo-respiration phytoplankton DO loss (prc) [no units]	0.014

ORGANIC PARTICLES (POM)	
Max transfer of POCL->DOCL (POC1max) [/day]	0.0100
Max transfer of POCR->DOCR (POC2max) [/day]	0.0005
Max transfer of POPL->DOPL (POP1max) [/day]	0.0500
Max transfer of POPR->DOPR (POP2max) [/day]	0.0005
Max transfer of PONL->DONL (PON1max) [/day]	0.0100
Max transfer of PONR->DONR (PON2max) [/day]	0.0005

DISSOLVED ORGANICS (DOM)	
Max mineralisation of DOCL->DIC (DOC1max) [/day]	0.003
Max mineralisation of DOCR->DIC (DOC2max) [/day]	0.0005
Max mineralisation of DOPL->PO_4 (DOP1max) [/day]	0.007
Max mineralisation of DOPR->PO_4 (DOP2max) [/day]	0.0005
Max mineralisation of DONL->NH_4 (DON1max) [/day]	0.007
Max mineralisation of DONR->NH_4 (DON2max) [/day]	0.0005

Nitrification/Denitrification	
Temp multiplier for denitrification (vN2) []	1.08
Denitrification rate coefficient (koN2) [/day]	0.40
Half sat const for denitrification (KN2) [mg/L]	0.30
Temp multiplier for nitrification (vON) []	1.08
Nitrification rate coefficient (koNH) [/day]	0.20
Half sat constant for nitrification (KOn) [mg O/L]	4.00
Ratio of O_2 to N for nitrification (YNH) [mg N/mg O]	3.42857

References

Alexander, R., & Imberger, J. (2008). Spatial distribution of motile phytoplankton in a stratified reservoir: the physical controls on patch formation. *Journal of Plankton Research*, *31*(1), 101–118. http://doi.org/10.1093/plankt/fbn101

Alldredge, A. L., Cowles, T. J., MacIntyre, S., Rines, J. E. B., Donaghay, P. L., Greenlaw, C. F., … Zaneveld, J. R. V. (2002). Occurrence and mechanisms of formation of a dramatic thin layer of marine snow in a shallow Pacific fjord. *Marine Ecology Progress Series*, *233*, 1–12. http://doi.org/10.3354/meps233001

Anneville, O., & Leboulanger, C. (2001). Long-term changes in the vertical distribution of phytoplankton biomass and primary production in lake Geneva: A response to the oligotrophication. *Alti Associazione Italiana Oceanologia Limnologia*, *14*, 25–35.

Birch, D. A., Young, W. R., & Franks, P. J. S. (2008). Thin layers of plankton: Formation by shear and death by diffusion. *Deep Sea Research Part I: Oceanographic Research Papers*, *55*(3), 277–295. http://doi.org/10.1016/j.dsr.2007.11.009

Birch, D., Young, W., & Franks, P. (2009). Plankton layer profiles as determined by shearing, sinking, and swimming. *Limnology and Oceanography*, *54*(1), 397–399. http://doi.org/10.4319/lo.2009.54.1.0397

Bjornsen, P. K., & Nielsen, T. G. (1991). Decimeter scale heterogeneity in the plankton during a pycnocline bloom of Gyrodinium aureolum. *Marine Ecology Progress Series*, *73*(2–3), 263–267. http://doi.org/10.3354/meps073263

Bollens, S. M., Rollwagen-Bollens, G., Quenette, J. A., & Bochdansky, A. B. (2011). Cascading migrations and implications for vertical fluxes in pelagic ecosystems. *Journal of Plankton Research*, *33*(3), 349–355. http://doi.org/10.1093/plankt/fbq152

Carraro, E., Guyennon, N., Hamilton, D., Valsecchi, L., Manfredi, E. C., Viviano, G., … Copetti, D. (2012). Coupling high-resolution measurements to a three-dimensional lake model to assess the spatial and temporal dynamics of the cyanobacterium Planktothrix rubescens in a

medium-sized lake. *Hydrobiologia*, *698*(1), 77–95. http://doi.org/10.1007/s10750-012-1096-y

Casamitjana, X., Schladow, G., & Roget, E. (1993). The seasonal cycle of a groundwater dominated lake. *Journal of Hydraulic Research*, *31*(3), 293–306. http://doi.org/10.1080/00221689309498827

Casulli, V., & Cheng, R. T. (1992). Semi-implicit finite difference methods for three-dimensional shallow water flow. *International Journal for Numerical Methods in Fluids*, *15*(6), 629–648. http://doi.org/10.1002/fld.1650150602

Chaves, F. Í. B., Lima, P. D. F., Leitão, R. C., Paulino, W. D., & Santaella, S. T. (2013). Influence of rainfall on the trophic status of a brazilian semiarid reservoir. *Acta Scientiarum. Biological Sciences*, *35*(4), 505–511. http://doi.org/10.4025/actascibiolsci.v35i4.18261

Cheriton, O. M., McManus, M. A., Holliday, D. V, Greenlaw, C. F., Donaghay, P. L., & Cowles, T. J. (2007). Effects of mesoscale physical processes on thin zooplankton layers at four sites along the west coast of the U.S. *Estuaries and Coasts*, *30*(4), 575–590. http://doi.org/10.1007/BF02841955

Cheriton, O. M., McManus, M. A., Stacey, M. T., & Steinbuck, J. V. (2009). Physical and biological controls on the maintenance and dissipation of a thin phytoplankton layer. *Marine Ecology Progress Series*, *378*(2003), 55–69. http://doi.org/10.3354/meps07847

Cloern, J. E., Alpine, A. E., Cole, B. E., & Heller, T. (1992). Seasonal changes in the spatial distribution of phytoplankton in small, temperate-zone lakes. *Journal of Plankton Research*, *14*(7), 1017–1024.

Cowles, T. J. (2003). Planktonic layers: Physical and biological interactions on the small scale. In L. Seuront & P. G. Strutton (Eds.), *Handbook of scaling methods in aquatic ecology: Measurement, analysis, simulation* (pp. 31–49). CRC Press.

Cowles, T. J., Desiderio, R. A., & Carr, M. (1998). Small-scale planktonic structure: Persistence and trophic consequences. *Oceanography*, *11*(1), 4–9. http://doi.org/10.5670/oceanog.1998.08

Cruz-Pizarro, L., Basanta-Alves, A., Escot, C., Moreno-ostos, E., & George, G. (2005). Temporal and spatial variations in the quality of water in El Gergal reservoir, Seville, Spain. *Freshwater Forum*, *23*, 62–77.

Cullen, J. (1982). The deep chlorophyll maximum: comparing vertical profiles of chlorophyll. *Deep*

Sea Research Part B. Oceanographic Literature Review. http://doi.org/10.1016/0198-0254(82)90274-6

Dekshenieks, M. M., Donaghay, P. L., Sullivan, J. M., Rines, J. E. B., Osborn, T. R., & Twardowski, M. S. (2001). Temporal and spatial occurrence of thin phytoplankton layers in relation to physical processes. *Marine Ecology Progress Series*, *223*, 61–71. http://doi.org/10.3354/meps223061

Derenbach, J., Astheimer, H., Hansen, H., & Leach, H. (1979). Vertical Microscale Distribution of Phytoplankton in Relation to the Thermocline. *Marine Ecology Progress Series*, *1*, 187–193. http://doi.org/10.3354/meps001187

Dillon, T. M. (1982). Vertical overturns: A comparison of Thorpe and Ozmidov length scales. *Journal of Geophysical Research*, *87*(C12), 9601–9613. http://doi.org/10.1029/JC087iC12p09601

Durham, W. M., Kessler, J. O., & Stocker, R. (2009). Disruption of vertical motility by shear triggers formation of thin phytoplankton layers. *Science*, *323*(5917), 1067–70. http://doi.org/10.1126/science.1167334

Durham, W. M., & Stocker, R. (2012). Thin Phytoplankton Layers: Characteristics, Mechanisms, and Consequences. *Annual Review of Marine Science*, *4*(1), 177–207. http://doi.org/10.1146/annurev-marine-120710-100957

Eckart, C. (1948). An analysis of the stirring and mixing processes in incompressible fluids. *J. Mar. Res*, *7*(3), 265–275.

Elliott, A., Escot, C., Basanta-Alves, A., & Cruz-Pizarro, L. (2005). Simulations of phytoplankton dynamics in El Gergal reservoir, southern Spain (PROTECH). *Freshwater Forum*, *23*, 78–92.

EPM. (2005). *Revista Hidrometeorológica Empresas Públicas de Medellín*. Medellín.

Eriksen, C. C. (1978). Measurements and models of fine structure, internal gravity waves, and wave breaking in the deep Ocean. *Journal of Geophysical Research*, *83*(C6), 2989. http://doi.org/10.1029/JC083iC06p02989

Fiedler, P. C. (1982). Zooplankton avoidance and reduced grazing responses to Gymnodinium splendens (Dinophyceae). *Limnology and Oceanography*, *27*(5), 961–965. http://doi.org/10.4319/lo.1982.27.5.0961

Fischer, H. B., List, J. E., Koh, C. R., Imberger, J., & Brooks, N. H. (1979). *Mixing in Inland and*

Coastal Waters. Academic Press.

Franks, P. (1992). Sink or swim, accumulation of biomass at fronts. *Marine Ecology Progress Series*, *82*, 1–12. http://doi.org/10.3354/meps082001

Franks, P. (1995). Thin layers of phytoplankton: A model of formation by near-inertial wave shear. *Deep-Sea Research Part I: Oceanographic Research Papers*, *42*(1), 75–91. http://doi.org/10.1016/0967-0637(94)00028-Q

Gallager, S. M., Yamazaki, H., & Davis, C. S. (2004). Contribution of fine-scale vertical structure and swimming behavior to formation of plankton layers on Georges Bank. *Marine Ecology Progress Series*, *267*, 27–43. http://doi.org/10.3354/meps267027

Genin, A., Jaffe, J. S., Reef, R., Richter, C., & Franks, P. J. S. (2005). Swimming Against the Flow: A Mechanism of Zooplankton Aggregation, *308*(May), 860–863.

George, D. G. (1993). Physical and chemical scales of pattern in freshwater lakes and reservoirs. *Science of the Total Environment, The*, *135*(1–3), 1–15. http://doi.org/10.1016/0048-9697(93)90271-7

George, D. G., & Edwards, R. W. (1976). The effect of wind on the distribution of chlorophyll A and crustacean plankton in a shallow eutrophic reservoir. *Journal of Applied Ecology*, *13*(3), 667–691. http://doi.org/10.2307/2402246

George, D. G., & Heaney, S. I. (1978). Factors influencing the spatial distribution in a small productive lake. *Journal of Ecology*, *66*(1), 133–155.

Gessner, F. (1948). The vertical distribution of phytoplankton and the thermocline. *Ecology*, *29*(3), 386–389. http://doi.org/10.2307/1931000

Gibson, C. H. (1980). Fossil temperature, salinity, and vorticity turbulence in the ocean. *Elsevier Oceanography Series*, *28*, 221–257. http://doi.org/10.1016/S0422-9894(08)71223-6

Gregg, M. C. (1987). Diapycnal mixing in the thermocline: A review. *Journal of Geophysical Research*, *92*(C5), 5249. http://doi.org/10.1029/JC092iC05p05249

Hillmer, I., Van Reenen, P., Imberger, J., & Zohary, T. (2008). Phytoplankton patchiness and their role in the modelled productivity of a large, seasonally stratified lake. *Ecological Modelling*, *218*(1–2), 49–59. http://doi.org/10.1016/j.ecolmodel.2008.06.017

Hipsey, M. ., Antenucci, J. ., & Hamilton, D. (2012). *Computational Aquatic Ecosystem Dynamics Model : CAEDYM v3*.

Hodges, B., & Dallimore, C. (2012a). Estuary , Lake and Coastal Ocean Model : ELCOM v2 . 2 Science Manual.

Hodges, B., & Dallimore, C. (2012b). *Estuary , Lake and Coastal Ocean Model: ELCOM*.

Holliday, D. ., Pieper, R. ., Grennlaw, C. ., & Dawson, J. . (1998). Acoustical sensing of small-scale vertical structures in zooplankton assemblages. *Oceanography*, *11*(1).

Holliday, D. V, Donaghay, P. L., Greenlaw, C. F., Mcgehee, D. E., Mcmanus, M. M., Sullivan, J. M., & Miksis, J. L. (2003). Advances in defining fine-and micro-scale pattern in marine plankton. *Aquatic Living Resources*, *16*, 131–136. http://doi.org/10.1016/S0990-7440(03)00023-8

Huisman, J., Van Oostveen, P., & Weissing, F. J. (1999). Species Dynamics in Phytoplankton Blooms: Incomplete Mixing and Competition for Light. *The American Naturalist*, *154*(1), 46–68. http://doi.org/10.1086/303220

Hutchinson, P. A., & Webster, I. T. (1994). On the distribution of blue-green algae in lakes: Wind-tunnel tank experiments. *Limnology and Oceanography*, *39*(2), 374–382. http://doi.org/10.4319/lo.1994.39.2.0374

Imberger, J. (1977). On the validity of water quality models for lakes and reservoirs. *Proc. 17th Cong. of the IAHR, Baden-Baden*.

Imberger, J. (1985). The diurnal mixed layer. *Limnology and Oceanography*, *30*(4), 737–770. http://doi.org/10.4319/lo.1985.30.4.0737

Imberger, J., Bermun, T., Christian, R. R., Sherr, E. B., Whitney, D. E., Pomeroy, L. R., … Wiebe, W. J. (1983). The influence of water motion on the distribution and transport of materials in a salt marsh estuary. *Limnology and Oceanography*, *28*(282), 201–214.

Imberger, J., & Patterson, J. (1980). Dynamic Reservoir Simulation Model- DYRESM: 5. In *Transport Models for Inland and Coastal Waters: Proceedings of a Symposium on Predictive Ability* (pp. 310–361). Academic Press New York.

Imberger, J., & Patterson, J. C. (1989). *Physical limnology*. *Advances in Applied Mechanics* (Vol. 27). Elsevier. http://doi.org/10.1016/S0065-2156(08)70199-6

Imboden, D. M. (1992). The impact of physical processes on algal growth. In David W. Sutcliffe And J. Gwynfryn Jones (Ed.), *Eutrophication: Research and application to water supply*. The Ferry House, Far Sawrey, Ambleside: Freshwater Biological Association.

Itsweire, E. C., Koseff, J. R., Briggs, D. A., & Ferziger, J. H. (1993). Turbulence in Stratified Shear

Flows: Implications for Interpreting Shear-induced Mixing in the Ocean. *Journal of Physical Oceanography*. http://doi.org/10.1175/1520-0485(1993)023<1508:TISSFI>2.0.CO;2

Itsweire, E. C., Osborn, T. R., & Stanton, T. P. (1989). Horizontal distribution and characteristics of shear layers in the seasonal thermocline. *Journal of Physical Oceanography*, *19*(3), 301–320. http://doi.org/10.1175/1520-0485(1989)019<0301:HDACOS>2.0.CO;2

Ivey, G. N., & Imberger, J. (1991). On the nature of turbulence in a stratified fluid. Part I: The energetics of mixing. *Journal of Physical Oceanography*, *21*(5), 650–658. http://doi.org/10.1175/1520-0485(1991)021<0650:OTNOTI>2.0.CO;2

Jenkinson, I. R., & Biddanda, B. A. (1995). Bulk-phase viscoelastic properties of seawater relationship with plankton components. *Journal of Plankton Research*, *17*(12), 2251–2274. http://doi.org/10.1093/plankt/17.12.2251

Laval, B., Hodges, B., & Imberger, J. (2003). Numerical diffusion in 3D, hydrostatic, z-level lake models. *Hydraul. Eng*, *129*(3), 215–224.

Lawrence, G. A., Ashley, K. I., Yonemitsu, N., & Ellis, J. R. (1995). Natural dispersion in a small lake. *Limnology and Oceanography*, *40*(8), 1519–1526. http://doi.org/10.4319/lo.1995.40.8.1519

Leonard, B. P. (1991). The ULTIMATE conservative difference scheme applied to unsteady one-dimensional advection. *Computer Methods in Applied Mechanics and Engineering*, *88*(1), 17–74. http://doi.org/10.1016/0045-7825(91)90232-U

Lévy, M. (2008). The modulation of biological production by oceanic mesoscale turbulence. In *Transport and Mixing in Geophysical Flows* (Vol. 744, pp. 165–218). http://doi.org/10.1007/978-3-540-75215-8

Lewis, W. M. (1987). Tropical limnology. *Annual Review of Ecology and Systematics*, *18*(1), 159–184. http://doi.org/10.1146/annurev.es.18.110187.001111

Lorenzen, C. J. (1967). Vertical distribution of chlorophyll and phaeo-pigments: Baja California. *Deep Sea Research and Oceanographic Abstracts*, *14*(6), 735–745. http://doi.org/10.1016/S0011-7471(67)80010-X

McManus, M. A., Alldredge, A. L., Barnard, A. H., Boss, E., Case, J. F., Cowles, T. J., … Zaneveld, J. R. (2003). Characteristics, distribution and persistence of thin layers over a 48 hour period. *Marine Ecology Progress Series*, *261*, 1–19. http://doi.org/10.3354/meps261001

McManus, M. A., Cheriton, O. M., Drake, P. J., Holliday, D. V., Storlazzi, C. D., Donaghay, P. L., &

Greenlaw, C. F. (2005). Effects of physical processes on structure and transport of thin zooplankton layers in the coastal ocean. *Marine Ecology Progress Series*, *301*(October), 199–215. http://doi.org/10.3354/meps301199

McManus, M. A., Kudela, R. M., Silver, M. W., Steward, G. F., Donaghay, P. L., & Sullivan, J. M. (2008). Cryptic blooms: Are thin layers the missing connection? *Estuaries and Coasts*, *31*(2), 396–401. http://doi.org/10.1007/s12237-007-9025-4

Menden-Deuer, S. (2008). Spatial and temporal characteristics of plankton-rich layers in a shallow, temperate fjord. *Marine Ecology Progress Series*, *355*, 21–30. http://doi.org/10.3354/meps07265

Miles, J. W. (1961). On the stability of heterogeneous shear flows. *Fluid Mech*, 496–508.

Mitchell, J. G., Yamazaki, H., Seuront, L., Wolk, F., & Li, H. (2008). Phytoplankton patch patterns: Seascape anatomy in a turbulent ocean. *Journal of Marine Systems*, *69*(3–4), 247–253. http://doi.org/10.1016/j.jmarsys.2006.01.019

Moline, M. A., Benoit-Bird, K. J., Robbins, I. C., Schroth-Miller, M., Waluk, C. M., & Zelenke, B. (2010). Integrated measurements of acoustical and optical thin layers II: Horizontal length scales. *Continental Shelf Research*, *30*(1), 29–38. http://doi.org/10.1016/j.csr.2009.08.004

Moreno-Ostos, E., Cruz-Pizarro, L., Basanta-Alvés, A., Escot, C., & George, D. G. (2006). Algae in the motion: Spatial distribution of phytoplankton in thermally stratified reservoirs. *Limnetica*, *25*(1–2), 205–216.

Moreno-Ostos, E., Cruz-Pizarro, L., Basanta, A., & Glen George, D. (2008). The spatial distribution of different phytoplankton functional groups in a Mediterranean reservoir. *Aquatic Ecology*, *42*(1), 115–128. http://doi.org/10.1007/s10452-007-9087-1

Moreno-Ostos, E., Cruz-Pizarro, L., Rueda, F., Escot, C., & Basanta-Alvés, A. (2005). *VI Simposio del Agua en Andalucía*. (Juan Antonio López Geta, J. C. Rubio Campos, & M. Martín Machuca, Eds.). Sevilla: Instituto Geológico y Minero de España.

Moreno Ostos, E. (2004). *Spatial dynamics of phytoplankton in el Gergal reservoir (Seville, Spain)*. [s.n.], Granada.

Nielsen, T. G., Kiørboe, T., & Bjørnsen, P. K. (1990). Effects of a Chrysochromulina polylepis subsurface bloom on the planktonic community. *Mar. Ecol. Prog. Ser.*

Osborn, T. (1998). Finestructure, microstructure, and thin layers. *Oceanography*, *11*(1), 36–43.

Osborn, T. R. (1980). Estimates of the local rate of vertical diffusion from dissipation measurements. *American Meteorological Society*, *10*, 83–89.

Osborn, T. R. (1988). Signatures of doubly diffusive convection and turbulence in an intrusive regime. *Journal of Physical Oceanography*, *18*(1), 145–155.

Prairie, J. C., Franks, P. J. S., & Jaffe, J. S. (2010). Cryptic peaks: Invisible vertical structure in fluorescent particles revealed using a planar laser imaging fluorometer. *Limnology and Oceanography*, *55*(5), 1943–1958. http://doi.org/DOI 10.4319/lo.2010.55.5.1943

Prairie, J. C., Franks, P. J. S., Jaffe, J. S., Doubell, M. J., & Yamazaki, H. (2011). Physical and biological controls of vertical gradients in phytoplankton. *Limnology & Oceanography: Fluids & Environments*, *1*, 75–90. http://doi.org/10.1215/21573698-1267403

Redfield, A. C. (1934). On the proportions of organic derivations in sea water and their relation to the composition of plankton. In *James Johnstone memorial volume* (p. 17). University Press of Liverpool.

Reynolds, C. S. (1984). *The ecology of freshwater phytoplankton*. Cambridge University Press.

Rigosi, A. (2010). *Physical and Ecological processes in El Gergal Reservoir (Seville): effects on water quality*. Universidad de Granada.

Rines, J. E. B., Donaghay, P. L., Dekshenieks, M. M., Sullivan, J. M., & Twardowski, M. S. (2002). Thin layers and camouflage: Hidden Pseudo-nitzschia spp. (Bacillariophyceae) populations in a fjord in the San Juan Islands, Washington, USA. *Marine Ecology Progress Series*, *225*, 123–137. http://doi.org/10.3354/meps225123

Robson, B. J., & Hamilton, D. P. (2004). Three-dimensional modelling of a Microcystis bloom event in the Swan River estuary, Western Australia. *Ecological Modelling*, *174*(1–2), 203–222. http://doi.org/10.1016/j.ecolmodel.2004.01.006

Roldán Pérez, G., & Ramírez Restrepo, J. J. (2008). *Fundamentos de limnología neotropical*. Editorial Universidad de Antioquia.

Román-Botero, R. (2011). *Caracterización Espacio Temporal de la Estructura Térmica de un Embalse Tropical Poco Profundo, Abastecido Parcialmente por Bombeo*.

Romero, J., Antenucci, J., & Imberger, J. (2004). One- and three dimensional biogeochemical simulations of two differing reservoirs. *Ecological Modelling*, *174*, 143–160.

Ryan, J. P., McManus, M. A., Paduan, J. D., & Chavez, F. P. (2008). Phytoplankton thin layers

caused by shear in frontal zones of a coastal upwelling system. *Marine Ecology Progress Series*, *354*, 21–34. http://doi.org/10.3354/meps07222

Ryan, J. P., McManus, M. A., & Sullivan, J. M. (2010). Interacting physical, chemical and biological forcing of phytoplankton thin-layer variability in Monterey Bay, California. *Continental Shelf Research*, *30*(1), 7–16. http://doi.org/10.1016/j.csr.2009.10.017

Scotti, R. S., & Corcos, G. M. (1972). An experiment on the stability of small disturbances in a stratified free shear layer. *Journal of Fluid Mechanics*, *52*(3), 499. http://doi.org/10.1017/S0022112072001569

Serra, T., Vidal, J., Casamitjana, X., Soler, M., & Colomer, J. (2007). The role of surface vertical mixing in phytoplankton distribution in a stratified reservoir. *Limnology and Oceanography*, *52*(2), 620–634. http://doi.org/10.4319/lo.2007.52.2.0620

Sevadjian, J. C., McManus, M. A., & Pawlak, G. (2010). Effects of physical structure and processes on thin zooplankton layers in Mamala Bay, Hawaii. *Marine Ecology Progress Series*, *409*, 95–106. http://doi.org/10.3354/meps08614

Sonntag, S., & Hense, I. (2011). Phytoplankton behavior affects ocean mixed layer dynamics through biological-physical feedback mechanisms. *Geophysical Research Letters*, *38*(15), 1–6. http://doi.org/10.1029/2011GL048205

Stacey, M. T., McManus, M. A., & Steinbuck, J. V. (2007). Convergences and divergences and thin layer formation and maintenance. *Limnology and Oceanography*, *52*(4), 1523–1532. http://doi.org/10.4319/lo.2007.52.4.1523

Steinberg, C. E. W., & Gruhl, E. (1992). Physical measures to inhibit planktonic cyanobacteria. In David W. Sutcliffe And J. Gwynfryn Jones (Ed.), *Eutrophication: Research and application to water supply*. The Ferry House, Far Sawrey, Ambleside: Freshwater Biological Association .

Steinbuck, J. V., Genin, A., Monismith, S. G., Koseff, J. R., Holzman, R., & Labiosa, R. G. (2010). Turbulent mixing in fine-scale phytoplankton layers: Observations and inferences of layer dynamics. *Continental Shelf Research*, *30*(5), 442–455. http://doi.org/10.1016/j.csr.2009.12.014

Steinbuck, J. V., Stacey, M. T., McManus, M. A., Cheriton, O. M., & Ryan, J. P. (2009). Observations of turbulent mixing in a phytoplankton thin layer: Implications for formation, maintenance, and breakdown. *Limnology and Oceanography*, *54*(4), 1353–1368.

http://doi.org/10.4319/lo.2009.54.4.1353

Strickland J.D.H. (1968). A comparison of profiles of nutrient and chlorophyll concentrations taken from discrete depths and by contonious recording. *Limnology and Oceanography*, *13*, 388–391. http://doi.org/10.4319/lo.1968.13.2.0388

Sullivan, J. M., Donaghay, P. L., & Rines, J. E. B. (2010). Coastal thin layer dynamics: Consequences to biology and optics. *Continental Shelf Research*, *30*(1), 50–65. http://doi.org/10.1016/j.csr.2009.07.009

Sullivan, J. M., McManus, M. A., Cheriton, O. M., Benoit-Bird, K. J., Goodman, L., Wang, Z., … McFarland, M. (2010). Layered organization in the coastal ocean: An introduction to planktonic thin layers and the LOCO project. *Continental Shelf Research*, *30*(1), 1–6. http://doi.org/10.1016/j.csr.2009.09.001

Sullivan, J. M., Twardowski, M. S., Donaghay, P. L., & Freeman, S. A. (2005). Use of optical scattering to discriminate particle types in coastal waters. *Applied Optics*, *44*(9), 1667. http://doi.org/10.1364/AO.44.001667

Thorpe, S. A. (1977). Turbulence and mixing in a scottish loch. *Philosophical Transactions of the Royal Society of London. Series A, Mathematical and Physical Sciences*, *286*, 125–181.

Toja, J., Basanta, A., & Fernández-Ales, R. (1992). Factors controlling algal biomass in the complex of water supply reservoirs of Seville (Spain). *Limnetica*, *8*, 267–277.

Townsend, D. W., Bennett, S. L., & Thomas, M. A. (2005). Diel vertical distributions of the red tide dinoflagellate Alexandrium fundyense in the Gulf of Maine, *52*, 2593–2602. http://doi.org/10.1016/j.dsr2.2005.06.027

Velo-Suárez, L., Fernand, L., Gentien, P., & Reguera, B. (2010). Hydrodynamic conditions associated with the formation, maintenance and dissipation of a phytoplankton thin layer in a coastal upwelling system. *Continental Shelf Research*, *30*(2), 193–202. http://doi.org/10.1016/j.csr.2009.11.002

Vidal, J., Marcé, R., Serra, T., Colomer, J., Rueda, F., & Casamitjana, X. (2011). Localized algal blooms induced by river inflows in a canyon type reservoir. *Aquatic Sciences*, *74*(2), 315–327. http://doi.org/10.1007/s00027-011-0223-6

Vidal, J., Moreno-Ostos, E., Escot, C., Quesada, R., & Rueda, F. (2010). The effects of diel changes in circulation and mixing on the longitudinal distribution of phytoplankton in a canyon-

shaped Mediterranean reservoir. *Freshwater Biology*, *55*(9), 1945–1957. http://doi.org/10.1111/j.1365-2427.2010.02428.x

Vidal, J., Rigosi, A., Hoyer, A., Escot, C., & Rueda, F. J. (2014). Spatial distribution of phytoplankton cells in small elongated lakes subject to weak diurnal wind forcing. *Aquatic Sciences*, *76*(1), 83–99. http://doi.org/10.1007/s00027-013-0316-5

Vuorio, K., Nuottajärvi, M., Salonen, K., & Sarvala, J. (2003). Spatial Distribution of Phytoplankton and Picocyanobacteria in Lake Tanganyika in March and April 1998. *Aquatic Ecosystem Health & Management*, *6*(3), 263–278. http://doi.org/10.1080/14634980301494

Wang, Z., & Goodman, L. (2009). Evolution of the spatial structure of a thin phytoplankton layer into a turbulent field. *Marine Ecology Progress Series*, *374*(May), 57–74. http://doi.org/10.3354/meps07738

Zaneveld, J. R., & Pegau, W. S. (1998). A model for the reflectance of thin layers, fronts, and internal waves and its inversion. *Oceanography*, *11*(1), 44–47.